2023년 8월

박사학위 논문

Unravelling Aging through Autophagy and Artificial Intelligence

Graduate School of Chosun University

Department of Integrative Biological Science

Karthikeyan Vijayakumar

Unravelling Aging through Autophagy and Artificial Intelligence

자식포작용 및 인공 지능 모델을 이용한 노화 연구

2023년 8월 25일

조선대학교 대학원

글로벌바이오융합학과

카르띠케얀 비자야쿠말

Unravelling Aging through Autophagy and Artificial Intelligence

지도교수 조광원

이 논문을 이학 박사학위신청 논문으로 제출함

2023년 4월

조선대학교 대학원

글로벌바이오융합학과

카르띠케얀 비자야쿠말

카르띠케얀 비자야쿠말의 박사학위논문을 인준함

위원장 조선대학교 교 수 전택중 (인)

위 원 조선대학교 교 수 이준식 (인)

위 원 조선대학교 교 수 김정수 (인)

위 원 전남대학교 교 수 장철호 (인)

위 원 조선대학교 교 수 조광원 (인)

2023년 06월

조선대학교 대학원

TABLE OF CONTENTS

LIST OF FIGURES ..... **iv**

LIST OF TABLES ..... **v**

ABBREVIATIONS ..... **vi**

ABSTRACT ..... **vii**

초록 ..... **x**

I. INTRODUCTION **1**

1. Aging **2**
2. Autophagy **2**
3. Rolipram **3**
4. Biological clock **4**
5. Present study **5**

II. PART 1. Role of Autophagy in the Protection of Cells Against Aging and Age Related Stress **8**

Chapter 1: Autophagy: An Evolutionarily Conserved Process in the Maintenance of Stem Cells and Aging……. **9**

1. Autophagy Traces in Prokaryotes……. **9**
2. Autophagy in Primitive Eukaryotes…….. **10**
3. Autophagy in Eukaryotes: from Plants to mammals. **11**
4. Evolution of AMPK AND mTOR……. **13**
5. Stem Cell Maintenance by Autophagy…….. **17**
6. Discussion…….. **19**

Chapter 2: Restoring Autophagy Flux by Rolipram attenuates ototoxicity induced by Kanamycin and Furosemide..... **21**

1. Introduction……... **21**
2. Materials and methods……... **25**
3. Results……... **29**
4. Discussion…….. **38**

III. PART 2. DNA Methylation Aging Clock…. **41**

Chapter 1:Pan-Tissue Methylation Aging Clock: Recalibrated And A Method To Analyze And Interpret The Selected Features…….. **42**

1. Introduction……... **42**

2. Methods……. **44**

3. Results……... **49**

4. Discussion…….. **76**

IV. CONCLUDING REMARKS……... **80**

REFERENCES……... **83**

LIST OF FIGURES

Figure 1. A diagrammatic representation of the autophagy mechanism…….. **6**

Figure 2. A schematic representation of the evolution of proteins involved in autophagy and their function at each evolutionary stage…….. **14**

Figure 3. Schematic representation of the toxicity induced by Kanamycin and Furosemide and the protective effects of rolipram……... **24**

Figure 4. Ototoxic effect of kanamycin and furosemide and the protective effect of rolipram in Hei-OC1 cells…… **30**

Figure 5. Higher activity of autophagy upon rolipram treatment…… **33**

Figure 6. Rolipram could not protect the Hei-OC1 cells against the ototoxicity upon inhibition of autophagy……... **36**

Figure 7. The selection of the concentration of the siRNA to inhibit the autophagy process……. **37**

Figure 8. A graphical representation of the study flow…… **43**

Figure 9. Performance of the model on both training and test data…… **50**

Figure 10. Performance of the methylation clock on various different tissues…… **53**

Figure 11. Performance of the methylation clock on various different tissues, which have not used in the training data……... **54**

Figure 12. Change in the methylation pattern of the selected probes……... **59**

Figure 13. Selected CpG probes have been separated according to their p values... **60**

Figure 14. Pathway Enrichment analysis…… **62**

Figure 15. Comparison with known genes curated from different databases…….. **65**

Figure 16. Performance of the top 10 probes……... **72**

Figure 17. Analysis of the top 10 probes…… **75**

LIST OF TABLES

Table 1: The presence of various orthologs of the core Atg proteins in different groups of organisms…… **16**

Table 2: Details of the datasets used for the study……. **47**

Table 3: Showing the details of datasets used in the study…… **48**

Table 4: Showing the accuracy metrics of the model……. **51**

Table 5: Accuracy metrics of the model in various tissues…….. **55**

Table 6: Accuracy metrics of the model in various tissues that are not used in the training session…… **56**

Table 7: Showing the list of known aging related genes from GenAge and CellAge……... **66**

Table 8: Showing the probesID belonging to the genes that are already known to be responsible for aging and their ranks from recursive feature elimination…….. **68**

Table 9: Showing the accuracy metrics of the 10 probes…… **73**

Table 10: Recursive feature elimination selected 10 probes, their respective genes and the known gene function……. **74**

ABBREVIATIONS

AI	Artificial Intelligence
Atg	Autophagy related
AMP	Adenosine monophosphate
AMPK	AMP-activated protein kinase
cAMP	cyclic AMP
ERK	Extracellular signal-regulated kinase
FBS	Fetal bovine serum
Hei-OC1	House ear institute – Organ of Corti 1
HSC	Hematopoietic stem cell
LC3	Light chain 3
MAE	Mean Absolute Error
mTOR	Mammalian target of rapamycin
MTT	Methylthiozolyldiphenyl-tetrazolium bromide test
NSC	Neural stem cell
PDE4	Phosphodiesterase 4
RMSE	Root Mean Squared Error
ROS	Reactive Oxygen Species
SVZ	Sub ventricular zone
ULK1	Unc-51-like kinase 1

ABSTRACT

Unraveling Aging through Autophagy and Artificial Intelligence

Karthikeyan Vijayakumar

Advisor: Prof. Gwang-Won Cho, Ph.D.

Department of Integrative Biological Science

Graduate school of Chosun University

Autophagy is an evolutionarily conserved process that degrades and recycles defective organelles, toxic proteins, and various other aggregates on the cytoplasmic surface by sequestering them into autophagosomes which, then, fuse with lysosomes which degrade them. If these aggregates are not cleared, they accumulate and damage the cell resulting in cellular senescence and aging. Stem cells, with their capacity to differentiate, are crucial for tissue homeostasis. In addition to differentiation, the stemness of stem cells must be preserved. Recent studies in stem cells show the importance of autophagy in evading cellular senescence and restoring the lost cells.

In the part one of my study I have implemented this strategy over age related hearing loss. By activating autophagy mechanism in the cells during stress, I could able to protect the cell from induced stress. Failure of autophagy flux has been reported as a major factor that impair hearing sense during various ototoxic conditions. In this study I used rolipram to restore the autophagy flux, which was failed upon the treatment of kanamycin and furosemide. Upon dose dependent treatment of kanamycin and furosemide, I observed depletion in the viability of the Hei-OC1 cells. The treatment of rolipram has been

effective in retrieving the failed autophagy flux to protect the cells from the cytotoxicity. Previous studies by various groups have shown the positive role of autophagy in the protection of cells. I have also found the activation of autophagy upon rolipram treatment. Although to make sure that the protective effect is by autophagy I used an autophagy inhibitor choloroquine and also knocked down the *Atg7* gene which involves in the conversion of LC3 I to LC3 II. On the inhibition of autophagy the treatment of rolipram could not protect the Hei-OC1 cells. The results of my study confirms that the activation of the autophagy flux could alleviate the toxicity and the use of rolipram helped in the protection of the Hei-OC1 cell during cytotoxic conditions.

Though autophagy is a viable mechanism to prevent cells during stress and prolong their life span, it is indeed better to unravel the fundamentals of the aging mechanism. Therefore, in the second part of the study I used the cutting-edge Artificial intelligence (AI) technology to unravel the epigenetic patterns during aging process. The abundance of the biological data and the rapid evolution of the newer machine learning technologies have increased the epigenetics research in the last decade. This has enhanced the ability to measure the biological age of humans and different organisms via their omics data. DNA methylation array data are commonly used in the prediction of methylation age. Horvath clock has been adopted in various aging studies as a DNA methylation age predicting clock due to its higher accuracy and multi tissue prediction potential. In the current study, I have developed a pan tissue methylation-aging clock by using the publicly available illumina 450k and EPIC array methylation datasets. In doing that, I developed a highly accurate epigenetic clock, which predicts the age of multiple tissues with higher accuracy. I used elastic net regression with a 10 fold cross validation to train the model. The model's performance was evaluated by using numerous metrics. The elastic net regression model selected 6,761 probes as the best features. I have analyzed the selected probes for their biological relevance. I found that the epigenetic aging process starts around the chronological of 30 and also I observed slower aging rate in

centenarians. Upon analyzing the selected features further, I found out evidences, which support the Antagonistic pleiotropy theory of aging.

초록

자식포작용 및 인공 지능 모델을 이용한 노화 연구

카르띠케얀 비자야쿠말

지도교수 : 조광원

글로벌바이오융합학과

조선대학교 대학원

Autophagy 는 결함이 있는 세포소기관, 독성 단백질 및 다양한 기타 응집체를 Autophagosome 로 격리시킨 후, 리소좀과 결합하여 분해하고 재활용되는 진화적으로 보존된 과정이다. 만약 이 응집체들이 제거되지 않으면, 이들은 축적되어 세포를 손상시켜 결국에는 노화를 유발한다._줄기 세포는 분화 능력을 가지고 있으며 조직의 항상성에서 매우 중요하다. 분화와 더불어 줄기세포의 줄기세포능도 보존되어야 한다. 줄기 세포에 대한 최근 연구는 세포 노화를 피하고 손상된 세포를 회복하는 데 Autophagy 의 중요성을 보여준다.

내 연구의 1 부에서는 노화 관련 청력 손실에 대해 이 전략을 수행하였다. 스트레스를 받는 동안 세포 내에서 Autophagy 메커니즘이 활성화하면 유도된 스트레스로부터 세포를 보호할 수 있다. 다양한 청각 독성 조건에서 Autophagy flux 의 손상은 청각을 손상시키는 주요 요인으로 보고되었다. 이 연구에서 나는 카나마이신과 푸로세마이드로 치료한 후 손상된 Autophagy 플럭스를 복원하기 위해 Rolipram 을 사용했습니다. 카나마이신과 푸로세마이드를 농도 별로 처리 시 Hei-OC1 세포의 생존력이 고갈되는 것을 관찰했다. PDE4 억제제인

Rolipram 의 처리는 세포 독성으로부터 세포를 보호하기 위해 손상된 Autophagy flux 회복시키는데 효과적이었다. 나는 또한 rolipram 처리 시 autophagy 의 활성을 발견했다. Autophagy 에 의해 보호 효과가 있는 것인지 확인하기 위해, 나는 Autophagy 억제제인 Choloroquine 을 사용했으며 LC3 I 에서 LC3 II 로의 전환에 관여하는 Atg7 유전자도 넉다운하였다. 그 결과, Autophagy 억제한 Hei-OC1 세포에서는 Rolipram 에 의한 보호효과를 관찰할 수 없었다. 우리 연구의 결과는 autophagy flux 의 활성화가 독성을 완화할 수 있고, rolipram 사용은 세포독성 조건에서 Hei-OC1 세포를 보호하는데 도움이 된다는 것을 확인시켜준다.

본 Autophagy 가 스트레스로부터 세포를 보호하고 수명을 연장하는 실행 가능한 매커니즘으로 확인했지만, 노화의 기본 매커니즘을 밝혀내는 것은 매우 복잡하고 많은 지식을 요구한다. 따라서 연구의 2 부에서는 최첨단 인공 지능(AI) 기술을 사용하여 노화 과정에서 발생하는 후성유전학적 패턴을 분석했다. 지난 10 년 동안 많은 생물학적 정보와 최신 머신 러닝 기술의 급속한 발전은 후성유전학 연구를 증가시켰다. 이것은 오믹스 데이터를 통해 인간이나 다른 유기체의 생물학적 나이를 측정할 수 있는 능력을 향상시켰다. DNA 메틸화 어레이 데이터는 일반적으로 메틸화 연령 예측에 사용된다. 최초이자 일반적인 모델 중 하나인 Horvath clock 은 더 높은 정확도와 여러 조직의 예측 가능성으로 인해 DNA 메틸화 연령 예측 시계로 다양한 노화 연구에서 채택되었다. 현재 연구에서는 공개적으로 사용 가능한 illumina 450k 및 EPIC 어레이 메틸화 데이터 세트를 사용하여 pan tissue methylation-aging clock 를 개발했다. 그 과정에서 나는 많은 조직의 나이를 예측할 수 있을 만큼 진보된 매우 정확한 후생유전학적 시계를 개발했다. 모델을 훈련하기 위해 교차 검증과 함께 탄성 망

회귀를 사용했슴니다 또한 선택한 프로브의 생물학적 유의성에 대해 분석했다. 선택한 특성을 추가로 분석한 결과, 노화에 대한 길항적 다면발현 이론을 뒷받침하는 증거를 발견했다.

모델을 훈련하기 위해 10 배 교차 검증과 함께 elastic net regression 을 사용했다. 모델의 성능은 여러 지표를 사용하여 평가되었다. Elastic net regression 모델은 최상의 특징으로 6,761 개의 프로브를 선택했다. 선택한 프로브의 생물학적 관련성을 분석했다. 나는 후성적 노화 과정이 30 세 전후에 시작된다는 것을 발견했고 또한 100 세 이상에서 노화 속도가 느려지는 것을 관찰했다. 선택한 특징들을 더 자세히 분석한 결과, 길항 다발성 노화 이론을 뒷받침하는 증거를 발견했다.

I. Introduction

1. Aging

Aging is an unavoidable process, which takes place in all the living organisms. It is the process of constant decline of the physiological processes in a time dependent manner. There are several hallmarks of ageing like telomere shortening, cellular senescence and various others (López-Otín et al., 2013). These could be because of various factors such as cell division, oxidative stress, and defective DNA damage response proteins (Jackson & Bartek, 2009). The unspoiled maintenance of protein homeostasis is critical to sustaining the function and structure of the cell. At any given point in time, mammalian cells synthesize and assemble more than 10,000 functionally and structurally different proteins. As proteins are sensitive, fragile, and at risk of misfolding, protecting them in various conditions is a challenging task (Hipp et al., 2014). Three major mechanisms are involved in maintaining protein homeostasis: the molecular chaperones, the proteasome proteolytic system, and the lysosome autophagy proteolytic system (Hipp et al., 2014; Wong & Cuervo, 2010). Mechanisms that promote proteome homeostasis can be helpful in slowing down the aging process (Balch et al., 2008).

2. Autophagy

Autophagy is a catabolic process by which protein aggregates, lipids, and even damaged and worn out cell organelles, such as mitochondria, are degraded, and thereafter, recycled by the lysosome (Galluzzi et al., 2017). Figure 1 shows the detailed autophagy mechanism. A basal level of autophagy occurs during normal growth (Melendez & Neufeld, 2008). The higher activity of autophagy, as occurs during starvation, is an evolutionarily conserved process (Kaur & Debnath, 2015). During starvation, components that are degraded by autophagy are utilized by the cell for energy metabolism. The downregulation of autophagy throughout starvation results in rapid cell death (Boya et al., 2005). Activation and inhibition of autophagy are controlled by the adenosine

monophosphate (AMP) activated protein kinase (AMPK) and the mechanistic target of Rapamycin (mTOR) pathways, respectively. Autophagy is highly dependent on the assembly of the Atg family of proteins (Klionsky et al., 2003; Tsukada & Ohsumi, 1993). When the production of energy and reactive oxygen species (ROS) increases, AMPK is activated to clear the aggregates and the accumulation ROS.

The AMPK pathway regulates the formation of the ULK1 (Unc-51-like kinase 1) complex that triggers the activation of the autophagy specific Class III Phosphatidyl inositol 3 kinase (PI3K) complexes and initiates autophagy. Atg9 and its regulators, Atg2 and Atg18, act with the PI3K complex to form the phagophore that then forms the autophagosome with the help of two ubiquitin-like conjugation reactions. In the first conjugation reaction, Atg7 and Atg10 induce the formation of another conjugate of Atg5 to Atg12 which later assembles into a large multiprotein complex containing Atg 16-like 1 (Atg16l1). The second conjugation reaction is that of phosphatidylethanolamine to microtubule-associated protein light-chain 3 (LC3) by the sequential action of Atg3 and Atg7 to form the LC3-II, the autophagosome bound form of LC3. With the lipid delivery through the Atg9 and the continuous assembly by the earlier mentioned complexes, the autophagosomal membrane elongates and closes to form the autophagosome. After its formation, the autophagosome fuses with the lysosome through molecules such as LAMPs and RAB7 (Figure1). The lysosomal acidic hydrolases regulate the degradation of the autophagy cargo which is then recycled in the anabolic processes that sustain cellular homeostasis.

3. Rolipram

Rolipram is a type of medication known as a phosphodiesterase 4 (PDE4) inhibitor. Initially, it was explored as an antidepressant but was not widely prescribed clinically due to its side effects (Li et al., 2011). PDE4 is an enzyme that plays a role in regulating the

levels of cyclic AMP (cAMP) within cells. By inhibiting PDE4, the cellular levels of cAMP increase (Fertig & Bawellie, 2018). Research has indicated that elevated levels of cAMP can have a positive effect on the activation of a protein called ERK, which, in turn, stimulates the activity of autophagy through proteins like Beclin-1 and LC3 II (Ugland et al., 2011). Moreover, increased cAMP levels also regulate the activity of AMPK, which is an upstream regulator of the autophagy mechanism (Omar et al., 2009).

4. Biological clocks

The rate of aging differs from one organism to another and also in humans, people with the same age shows varied physical and health changes (Baker & Sprott, 1988). It is reasonable to estimate that DNA methylation could potentially be one of the factors to influence the rate of aging (Ferrucci et al., 2020). Therefore, the past decade has seen various researches trying to establish aging markers based on epigenetic changes. One such research is the establishment of clock based on the methylation pattern. This was achieved by the usage of machine learning algorithms. In the year 2013 Hannum developed a methylation age clock (Hannum et al., 2013) using a blood derived dataset with a higher prediction accuracy. However, the model has suffered when it was applied onto other tissues. In the same year Steve Horvath developed a methylation clock using multiple tissues with a near perfect accuracy and was known as DNAmage (Horvath, 2013). In the later years, several different epigenetics clocks were developed with as low as just 3 CpG sites (Lin et al., 2016). In order to predict the lifespan along with the DNA methylation data Levine et al included blood derived clinical markers and chronological age to develop the DNA PhenoAge (Levine et al., 2018). GrimAge (Lu et al., 2019), another clock model which utilizes smoking habit and plasma protein level was developed to predict the lifespan and the all-cause mortality. Both the clocks were better at predicting the lifespan and mortality factors when compared with the Horvath's clock, which only utilizes the methylation data.

5. Present study

This study is divided into two parts In the first part of the current study I have tracked the evolutionary path of the autophagy mechanism by analyzing the protein similarities. I have analyzed the similarities between the autophagy related protein in various species ranging from single to multicellular organisms. I have found out that autophagy is an evolutionarily conserved process which protects the cells during stress conditions. By adapting this knowledge I tested the cell protective effects of autophagy in a hearing loss model. By activating autophagy by the drug rolipram I was able to protect the cell death in the hearing loss model. This shows that drugs which targets the activation of autophagy may be therapeutically viable in treating hearing loss. Further, we wanted to explore more about the fundamental process of the aging process. We used the modern AI machine learning technology to predict the human age from the DNA methylation data. We used multiple tissues from age ranging from 0 to 103. Our clock model could accurately predicted the DNA methylation age. We also found that the CpG probes selected by the model are located on the genes which basically involves in various developmental pathways. This is one of the evidences for the antagonistic pleiotropy theory of aging. My current research involve both traditional molecular biology works to identify a mechanism to protect cells during aging related and toxic conditions and also the utilization of the modern AI to decode the molecular methods behind the aging process.

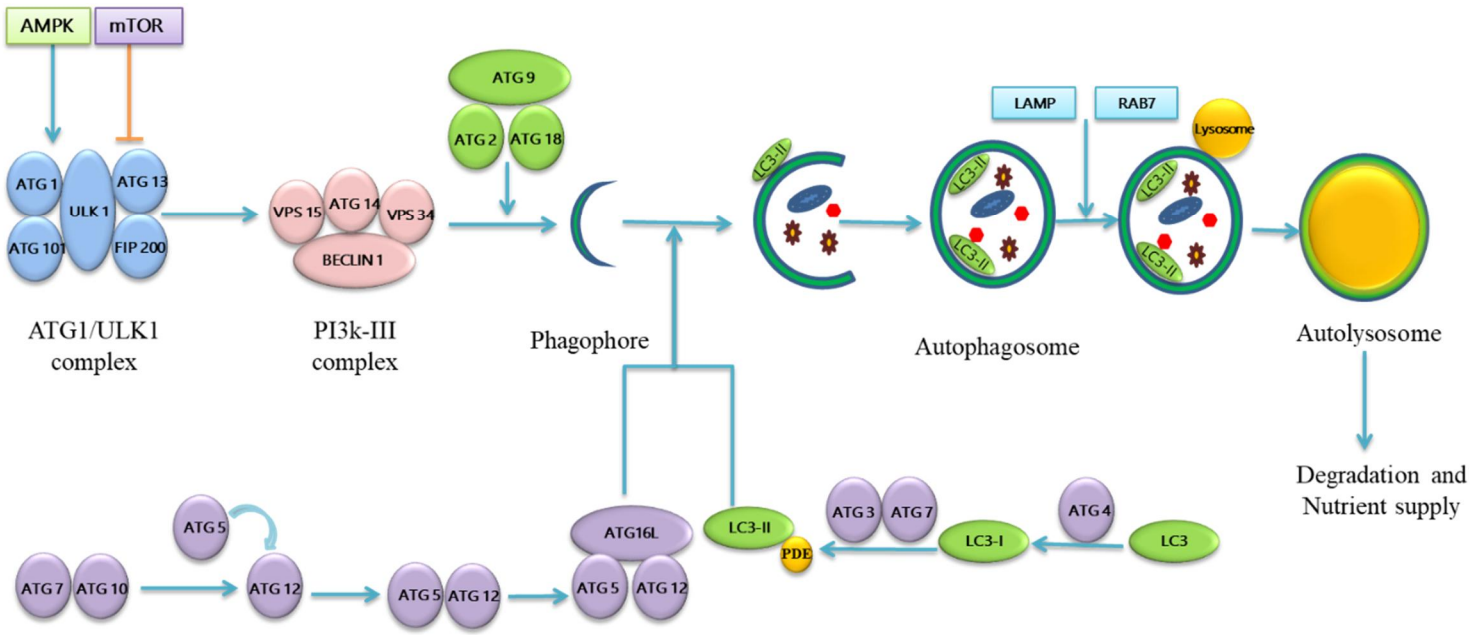

Figure 1. A diagrammatic representation of the autophagy mechanism. The AMPK and mTOR signaling pathways control the induction of autophagy. The assembly of the ULK1/Atg1 and PI3K complexes denotes the beginning of the autophagy process. This assembly supplies the membrane smyce for the formation of the phagophore. Two ubiquitin-like conjugation reactions are necessary for the formation of the autophagosome. One reaction involves the conjugation of Atg7 and Atg10 that induces the formation of a conjugate of Atg5 and Atg12, which then assembles into a large multiprotein complex containing Atg16L1. The other reaction involves the conjugation of

Figure 1.continued

Phosphatidylethanolamine to LC3 by the sequential action of Atg3 and Atg7 to form LC3-II. Lipid delivery through Atg9 allows the autophagosomal membrane to elongate and close to form the autophagosome. The autophagosome fuses with the lysosome through molecules such as LAMPs and RAB7. The autolysosome then degrades cargo and sustains cellular homeostasis.

II. Part 1: Role of Autophagy in the Protection of Cells Against Aging and Age Related Stress

Chapter 1

Autophagy: An Evolutionarily Conserved Process in the Maintenance of Stem Cells and Aging

1. Autophagy Traces in Prokaryotes

While almost all Atg proteins are evolutionarily conserved, some of them are present in either numerous copies or are missing entirely (Brennand et al., 2011; Duszenko et al., 2011). Although autophagy functions virtually in all eukaryotes, one cannot conclude that it suddenly evolved in them. Prokaryotes are primitive and one of the earliest formed organisms. Therefore, it is an appropriate approach to track the traces of autophagy through evolution beginning with prokaryotes. Evidences suggests the presence of some distant homologs of *Atg*s in cyanobacteria and euryarchaeota (Yang et al., 2017). Atg1/ULK1 is the first protein complex involved in the induction of autophagy. When looking for similar orthologs in prokaryotes, proteins resembling the serine/threonine kinases have been observed (Table 1). However, since prokaryotes neither have internal membranes nor lysosomes, the core autophagy process of forming autophagosomes and its conjugation with the lysosome, is absent. Hence, I deduce that the putative serine threonine kinase was involved in a different function such as in inducing proliferation in prokaryotes (Wang et al., 2017). It is conclusive that serine threonine kinase aids the prokaryotes in survival through proliferation as most of these primitive organisms thrive in extreme environments. As in their eukaryotic counterparts, bacterial cells need to maintain cellular homeostasis by degrading intracellular proteins and organelles (Pickart & Cohen, 2004). A degradation signal is embedded in the primary sequence of bacterial proteins that must be degraded. The proteins are then degraded by proteases. This shows

that the core autophagy mechanism of degradation have originated at a later point in evolution (Hughes & Rusten, 2007).

2. Autophagy in Primitive Eukaryotes

A comparative genomic study on the presence of the *Atg* genes in parasites such as *Entamoeba histolytica*, *Plasmodium yoelii*, *Trypanosoma brucei,* and *Encephalitozoon cuniculi* showed relatively less *Atg*s (Yang et al., 2017). In the protist, *E. histolytica,* the activity of autophagy in proliferation and differentiation has been reported (Picazarri et al., 2008). Orthologs of Atg proteins involved in the expansion and completion of vesicles were found in *Plasmodium falciparum*, whereas genes involved in either of the two ubiquitin-like conjugations required for the induction of autophagy and cargo delivery to lysosomes seem completely absent. Atg8 (LC3 in mammals), the marker for the autophagosome, is localized in the apicoplast (Cervantes et al., 2014). In *Plasmodium* parasites, Atg8 is involved in the fusion and segregation of the apicoplast during replication (Walczak et al., 2018). The BLAST analysis of the genome of *Encephalitozoon cuniculi* showed the absence of *Atg*12 and *Atg*8 (Katinka et al., 2001). This proves that in lower eukaryotes, the formation of autophagosome and the degradation of cargo are absent. The presence of a few Atg orthologs, such as serine threonine kinase and Phosphatidylinositol 3 Kinase (the orthologs of Atg1 and Atg13 of yeast) shows that autophagy is not completely developed in these organisms, and that these genes were involved in various other roles, especially in ubiquitination and cell division (Table 1). Most of these early eukaryotes are parasites which live within other organisms, thus their environments are nutritionally rich, and the role of autophagy in nutrition supply during starvation must have evolved in the later stages of evolution (Hughes & Rusten, 2007).

3. Autophagy in Eukaryotes: from Plants to Mammals

Atg genes were identified in plants such as *Arabidopsis,* rice, tomato, potato, barley, and wheat suggesting that the autophagy system is highly active in them (Doelling et al., 2002). Although some homologs of *Atg* genes involved in the initiation of autophagy have been seen in prokaryotes and primitive eukaryotes, the core *Atg* genes involved in the formation of autophagosomes are present only in the evolutionarily developed eukaryotes. In plants, the defects in autophagy lead to senescence and disproportionate immunity-related programmed cell death (PCD) irrespective of nutrient conditions (Liu et al., 2005). In the plant species, *Nicotiana benthamiana*, silencing the Atg6 gene resulted in reduction of autophagy activity and chlorotic cell death (Liu et al., 2005). In nutrient-rich conditions, it is reported that mutations in *Atg* genes lead to early senescence (Doelling et al., 2002). This may be because upon the activation of mTOR, rapid cell differentiation occurs. Atg7 is crucial for the conjugation of Atg8 and Atg12 (Figure 2), and a mutation of this gene in *Arabidopsis thaliana* showed accelerated senescence and sensitivity to low-nutrient conditions (Doelling et al., 2002). This proves that autophagy is involved in the supply of nutrients to the cells during starvation. The autophagy defective mutation of *Atg*2 and *Atg*5 in *Arabidopsis* resulted in early senescence and immunity-related PCD signifying that autophagy in plants plays a major role in the pro-survival function during the progression of cell death (Yoshimoto et al., 2009). A high level of accumulated salicylic acid was present in *Arabidopsis thaliana* with Atg5 mutations, and large quantities of senescence markers, such as SAG12, were expressed. The accumulation of salicylic acid corresponded with the accumulation of ROS (Yoshimoto et al., 2009). ROS accumulation is a major cause for cellular senescence (Jeong & Cho, 2015), and it is known that autophagy negatively regulates the accumulation of ROS. Accumulation of ROS triggers autophagy by activating AMPK (Filomeni et al., 2014). In yeast and mammals, dysfunctional mitochondria accumulate due to the lack of autophagy, leading to increased

ROS production (Zhang et al., 2007). The formation of Atg5 complex with Atg12 and Atg16L1 helps in the elongation of the autophagosome (Mizushima et al., 2002). In mice, the ROS buildup, due to the defect in *Atg*5 gene, reduced the stem cells and impaired the intestinal tissue homeostasis (Asano et al., 2017). Similar to the role of Atg8 in apicoplast segregation during cell division in lower eukaryotes, a functional homolog of LC3 is involved in a programmed mechanism in higher eukaryotes. This is independent of damage responses involved in the elimination of mitochondria during erythrocyte differentiation (Sandoval et al., 2008; SchIers et al., 2007). These evidences confirm the association between autophagy and the removal of excessive ROS and the degradation of defective mitochondria to maintain cellular senescence.

An increased ROS level disrupts cell homeostasis leading to cell death. Another research on Crohn's disease states that the cause of disease is associated with mutations in Atg16l1 (Rioux et al., 2007), a gene coding a protein that is responsible for the formation of the autophagosome. As seen in both humans and mice, the lack of Atg16l1 results in functional abnormalities in Paneth cells (CadWell et al., 2008; Marchiando et al., 2013). *Atg*7 is a major regulator of the adult hematopoietic stem cell (HSC) maintenance. Deleting *Atg*7 and constraining autophagy in HSC has resulted in the loss of normal function. Additionally, HSC display an accumulation of ROS and DNA damage (Mortensen et al., 2011). The loss of *Atg*7 also leads to neural degeneration. Notably, accumulation of polyubiquitinated proteins, accumulated in neurons deficient in autophagy, increases the size and number of aging cells (Komatsu et al., 2006). Inhibition of autophagy by targeting different steps in the formation of the autophagosome through various *Atg* genes in the primordial gut of *Drosophila* showed suppression of the autophagic degradation function (Nagy et al., 2018). Therefore, in eukaryotes, the regulation of every step of autophagy is vital to the integrity of tissue homeostasis and is responsible for controlling the organism's aging process.

4. Evolution of AMPK and mTOR

Both AMPK and mTOR belong to the protein kinase family of proteins (Mita et al., 2003). These signaling proteins are present in almost all higher eukaryotes. Although they are absent in prokaryotes, some proteins that resemble the serine threonine protein kinases can be seen in them (Table 1). In primitive prokaryotes, their involvement in cell division resembles the mTOR activity in cell division and differentiation. Cells need abundant energy to proliferate and differentiate to maintain homeostasis. Under insulin signaling, the mTOR pathway is activated and involves in the differentiation of stem cells, thereby, maintaining tissue homeostasis (Figure 2). mTOR forms two complexes, mTORC1 and mTORC2. The activity of mTORC1 depends on the cell's nutritional status. mTORC1 acts through the downstream target, S6 kinase (S6K) (Kim et al., 2002). mTOR inhibits ULK1 complex formation by phosphorylating serine residues. Since S6K is a downstream target of mTORC1, it is considered a negative regulator of autophagy. A study on the fat bodies of Drosophila revealed that TOR inhibited autophagy independent of S6K, and S6K was, in fact, required for starvation-induced autophagy (Scott et al., 2004). While autophagy recycles the cellular contents for survival, excessive autophagy can result in cell death. Thus, the roles of mTOR and S6K in autophagy balance the extent of autophagy during nutrient deprivation (Sridharan et al., 2011). AMPK activation leads to the upregulation of *Atg* genes (Chiacchiera & Simone, 2009). At the basal level, autophagy is activated when ROS accumulates by the phosphorylation of Atg1/ULK1 by AMPK (Figure 2), resulting in maintenance of the stem cell. The balance between the activities of AMPK and mTOR evolved for the survival of organisms.

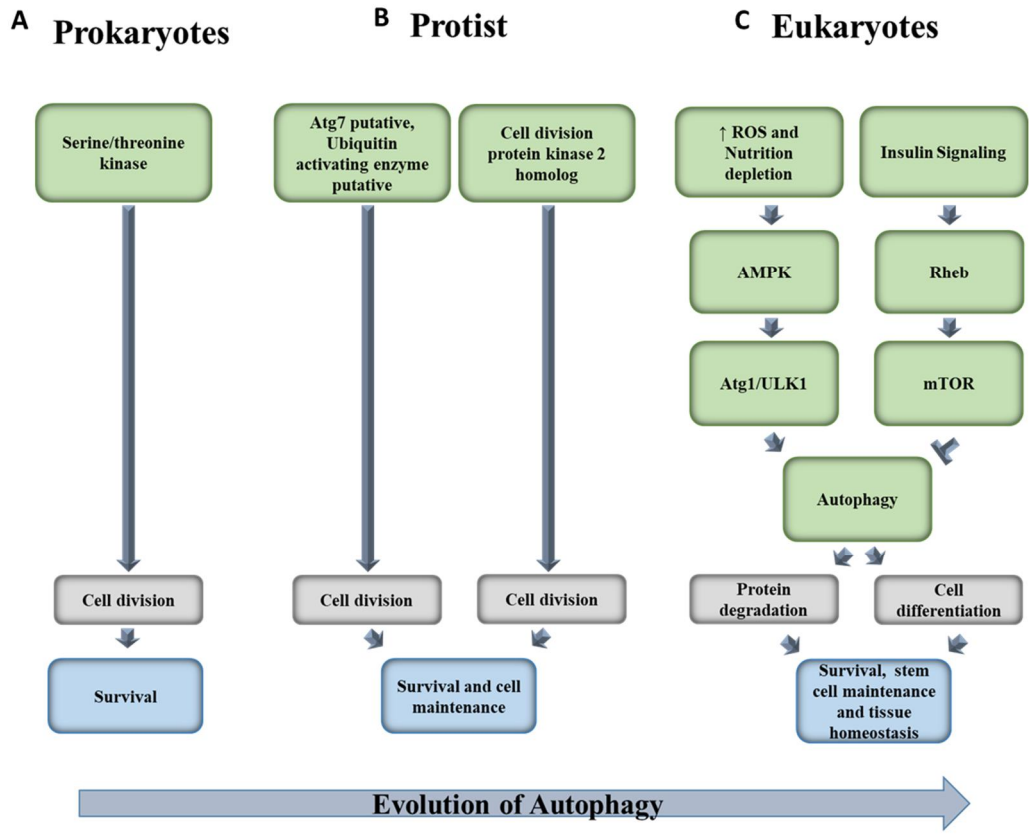

Figure 2. A schematic representation of the evolution of proteins involved in autophagy and their function at each evolutionary stage. (A) The evolution and function of the Atg in Prokaryotes. The BLAST analysis shows that serine/threonine kinase is a distant ortholog of Atg1. It is involved in the cell cycle. (B) In primitive prokaryotes, especially protists, along with the homolog of Atg1, other homologs, such as Atg7 putative and ubiquitin-activating enzyme putative, are also present and are involved in the ubiquitination of proteins. Comparative protein analysis shows the presence of the Phosphatidylinositol 3-kinase Tor2 putative, a homolog of TOR. This assists in the proliferation of cells and the survival of the organism by maintaining its population. (C) The function of autophagy in eukaryotes. A constant and high supply of nutrition causes

the activation of Rheb. This, in turn, activates the mTOR signaling pathway. mTOR activates mTORC1, which phosphorylates Atg1/ULK1 and inhibits autophagy, resulting

Figure 2. Continued

in stem cell differentiation. When nutrition depletes and ROS accumulate, AMPK is activated. AMPK bypasses the phosphorylation of mTORC1 and directly phosphorylates Atg1/ULK1 and induces autophagy resulting in the degradation of the aggregates and in stem cell proliferation

Table 1: The presence of various orthologs of the core Atg proteins in different groups of organisms.

***Atg* Genes (*S. cerevisiae*)**	**Prokaryotes**	**Protists**	**Plants**	**Invertebrates**	**Vertebrates**
Atg1	Serine threonine protein kinase A	Cell division protein kinase 2 homolog	Atg1	Atg1	ULK1
Atg7	-	Atg7 putative, Ubiquitin activating enzyme putative	E1 C-terminal related, ThiF family protein	Atg7	Atg7
Atg8	-	-	Ubiquitin-like superfamily protein, Autophagy 8E	Atg8a, Atg8b	LC3, Gamma-aminobutyric acid receptor-associated protein
Atg12	-	-	Ubiquitin-like superfamily protein	Atg12	Atg12
TOR1 and 2	-	Phosphatidylinositol-3-kinase Tor-2, putative	Target of Rapamycin	Target of rapamycin	mTOR

5. Stem Cell Maintenance by Autophagy

The stem cell pool in an organism reduces with aging. This is proven by various studies done on different stem cells. The sub ventricular zone (SVZ), in the forebrain of a mouse or rat, consists of neural stem cells (NSC). A decrease in the number of NSC in the SVZ results in the impairment of neurogenesis (Enwere et al., 2004). Similarly, the number of cells in the mesenchymal stem cell pool also reduces with aging (Oliver et al., 2012). This might be because of the autophagic flux in the young cells. Autophagic flux refers to the entire mechanism of autophagy until the degradation process (Ferraro & Cecconi, 2007). In HSC, the loss of autophagy during an overactive metabolic state results in the loss of quiescence and accelerated differentiation (Ho et al., 2017). In muscle cells, a constructive autophagic activity can be seen in young quiescent cells, whereas the autophagic activity impairs with age. This can also be seen in the SVZ of the rat brain where protein degradation in quiescent NSC involved autophagy, whereas in activated NSC, proteasome-mediated protein degradation was involved. This proves that autophagy is involved in maintaining quiescent stem cells and in stem cell proliferation.

Autophagy works as an additional mechanism that responds to the energy demand of stem cell proliferation, whereas other energy metabolic pathways, such as glycolysis and insulin signaling pathways, lead to the activation of mTOR which, in turn, leads to the differentiation, rather than proliferation, of stem cells (Oliver et al., 2012). Autophagy digests the protein aggregates and supplies the energy required for quiescent stem cells to proliferate, thus maintaining pristine proteomes inside the cell. This process results in maintaining the stemness of stem cells and delays stem cell senescence. One of the essential functions of autophagy is to degrade mitochondria. This action controls the oxidative metabolism, thereby maintaining the stemness and the potential to regenerate (Kim et al., 2011).

The restriction of nutrients is a trending way to prolong the aging process as autophagy is activated during starvation. Inhibition of mTOR is also known to activate autophagy (Figure 1). mTOR can be inhibited by the usage of pharmaco-chemicals. Rapamycin, an mTOR inhibitor, aids in the enhancement of the lysosome-autophagy pathway. Several derivatives of Rapamycin (rapalogs), such as Temsirolimus, Ridaforolimus, and Zotarolimus, have also shown promising results in inhibiting mTOR. Metformin, an FDA approved drug, is an activator of AMPK. It also regulates mTOR through the inhibition of Ras-related guanosine triphosphate binding (Lamming et al., 2013). As new drugs are discovered in a rapid manner, it is possible to prolong the aging process.

6. Discussion

When I look at the evolution of autophagy, the core autophagy process (the formation of the two ubiquitin-like conjugations) and the *Atg* genes involved in this process are crucial in higher eukaryotes. Although autophagy and the *Atg* genes are evolutionarily conserved, *Atg*3, *Atg*5, *Atg*7, *Atg*8, and *Atg1*2 are involved in the formation of the autophagosome, which is unique to eukaryotes. One major difference between prokaryotes and eukaryotes is the presence of major membrane bound organelles in the eukaryotic cells, especially the mitochondria. Studies show that mitochondria are derived from early proteobacteria that formed an endosymbiotic relationship with higher eukaryotes (Muller et al., 2012). Although mitochondria are helpful in cell survival, their numbers have to be maintained as the number of mitochondria present is directly proportional to the production of ROS, a major cause of senescence of cells (Kuilman et al., 2010).

The BLAST results point out that the distant homologs of the *Atg* genes of primitive eukaryotes, serine threonine kinases, are involved in the proliferation of cells. Some bacteria living in extreme conditions also have these homologs. These *Atg* genes were acting as survival guides for those organisms to maintain their population. Autophagy is also involved in innate immunity (Deretic, 2012). Intracellular bacterial pathogens, such as *Shigella* and *Streptococcus*, multiply in the cytoplasm after evading the phagosome or endosome. Autophagy counteracts these infections by recapturing and degrading the bacteria (Nakagawa et al., 2004). The involvement of autophagy in innate immunity might have evolved after the symbiotic relationship between mitochondria and eukaryotic cells developed. mTOR signaling is another important regulator of autophagy and cell division. Homologs of mTOR in primitive organisms match PI3K. During evolution, the autophagy genes involved in cell survival by inducing cell proliferation developed the mechanism of mTOR and autophagy lysosome degradation during conditions including low nutrient supply, organelles damage, and ROS accumulation. These mechanisms aid

in the survival of the organism. Therefore, it can be noted that autophagy and mTOR signaling constitute one complex mechanism which evolved together for the survival of the organism for either maintaining stem cells or for differentiating cells to maintain tissue homeostasis.

Chapter 2

Restoring Autophagy Flux by Rolipram Attenuates Ototoxicity Induced by Kanamycin and Furosemide.

1. Introduction

Hearing loss is one of the concerning factors that affects a person's quality of life. Among all the hearing loss patients 74.6% patients shows sensorineural damage (Martines et al., 2010). There are numerous reasons like loud noise, aging and administration of ototoxic drugs that are responsible for the sensorineural damage (Fetoni et al., 2013; Nayagam et al., 2011). The sensorineural damage denotes the loss of the epithelial cells i.e., Inner Hair cells or the Outer hair cells (Hong et al., 2013). This loss of the hair cells leads to a cycle of misfortunate events that progress into damaging the auditory cortex eventually causing hearing loss. Unlike the lower organisms it is unlikely for the mammalian hair cells to regrow the lost hair cells (Roberson & Rubel, 1994). Upon maturation, the auditory sensory epithelium loses its ability to regenerate their lost hair cells and also the vestibular sensory epithelia supports only a partial regenerative response to trauma (Kawamoto et al., 2009; Lin et al., 2011). The death of outer hair cells or the inner hair cells or the rupture of the basilar membrane leads to a decrease in neuronal output from the cochlea to the brain. To assimilate sensorineural hearing loss, it is crucial to prevent or alleviate the degeneration of cochlear nerve fibers and spiral ganglion neurons (SGN) upon the loss of sensory hair cell.

Autophagy is a scavenging process, which clears all the unwanted aggregates and damaged organelles so that the cell surface is maintained in a pristine condition (Stacchiotti & Corsetti, 2020). It has been proved that the activation of autophagy during

neomycin and gentamycin treatment, leads to the delayed ototoxicity and also the ototoxicity is because of the overproduction of ROS caused by excitotoxicity (He et al., 2017). Autophagy is also remove the damaged mitochondria (Ding & Yin, 2012), that is responsible for the overproduction of ROS. Impaired autophagy flux have been seen to cause cell death including neuronal cell death (Sarkar et al., 2014; Singh et al., 2014). Numerous different pathways regulates the autophagy mechanism including AMP-activated protein kinase (AMPK) and extracellular signal-regulated kinase (ERK) pathway (Meijer & Codogno, 2004, 2009; Ravikumar et al., 2010). Recent studies by various groups has shown the activation of autophagy upon various ototoxic conditions and the failure of the completion of autophagy flux has been observed in these studies (He et al., 2017; Kim et al., 2017). In this study I wanted to utilize activation of autophagy to protect the cells from ototoxic conditions.

Researchers have been using different *in-vitro* models to study hearing loss. It is Well known that aminoglycosides are major ototoxic drugs (Kotecha & Richardson, 1994; Sun et al., 2014). In earlier researches Kanamycin – an aminoglycoside which has been administered along with ethacrynic acid to damage the sensory epithelial cells in the guinea pig's inner ear to establish a SGN degeneration model (Bock et al., 1983). In order to simulate the pathological changes of the sensorineural hearing loss in cochlea Bin Ye et al (Ye et al., 2019) used kanamycin and furosemide to establish a mouse model for the sensorineural hearing loss. As observed in another study, kanamycin does not damages the hair cells and nerve fibers like gentamycin (Ruan et al., 2014). The treatment of kanamycin and furosemide emulated the damaging pattern of SGN of that of most of the sensorineural hearing loss patients. Therefore I adopted the treatment of kanamycin and furosemide to establish the hearing loss model for my study.

In one of my previous unpublished studies I have observed the activation of autophagy in rat fetal neural stem cells upon rolipram treatment. Therefore in the current study I wanted

to prevent the Hei-OC1 cells against the kanamycin and furosemide (K+F) induced cytotoxicity by the activation of autophagy with rolipram. In Figure 3 I have shown the detailed mechanism behind the K+F toxicity and the protective mechanism of rolipram by activating autophagy. In my current study I have rectified the failed autophagy flux using rolipram. This have resulted in the protection of Hei-OC1 cells.

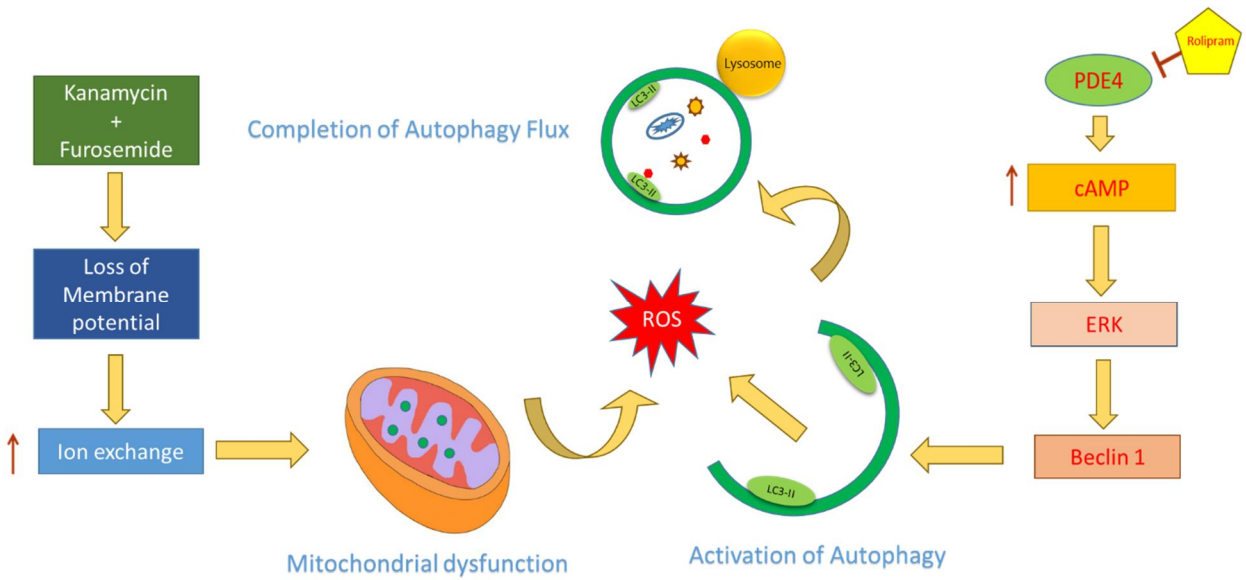

Figure 3. Schematic representation of the toxicity induced by Kanamycin and Furosemide and the protective effects of rolipram. Administration of K+F causes loss of membrane potential in the cells resulting in increased ion exchange. This causes mitochondrial dysfunction and produces ROS causing cell death. Rolipram administration increases cAMP production and activates ERK pathway. ERK is known to stimulate Beclin1 and thus activates autophagy. Upon the completion of autophagy flux all the damaged organelles and ROS were removed from the cell and prevents cell death.

2. Materials and methods

Cell culture and treatment

Hei-OC1 cells were cultured at 33° C with 5% CO_2 in DMEM high glucose media (Gibco, USA) supplemented with 10% fetal bovine serum (Gibco, Canada). Antibiotics were not added to the media as they are toxic to the cell line. Cells were sub-cultured once 80% confluence has been reached. Once the cells gets attached to the plate surface, the media was removed and the cells were washed with 1XPBS. The cells were then treated with 0.1μM rolipram for the next 48hours. After 48 hours treatment the media was removed and cells were once again washed. 30μM kanamycin sulfate and 3μM furosemide were added. The cells were then kept in 33°C for the next 24hours and further experiments were conducted.

MTT assay

For the MTT assay, cells were seeded in a 96 Well plate. Once the treatments were done the media was removed and washed one time with 1 X PBS. 5mg/mL 3-(4,5-dimethylthiazol-2-yl)-2,5-diphenyltetrazolium bromide or MTT solution was added to the cells and incubated in 37° C for 2 hours. Later the MTT solution was removed and the deposition of formazon was dissolved in DMSO. Then the cell viability was measured at 560nM wavelength using a microplate reader.

CYTO-ID staining

To check the autophagy activity upon the treatment of rolipram CYTO-ID autophagy detection kit (enzo) was used. Hei-OC1 cells were grown upon poly D-Lysine (Thermo Fisher Scientific, Waltham, MA, USA) coated coverslips. Rapamycin was used as a positive control for autophagy. In order to measure the autophagy flux chloroquine was used to block the lysosomal activity. In this way the autophagosomes gets accumulated

and autophagy activity can be visualized. Once the treatments were done the cells were washed and the CYTO-ID stain was added according to the manufacturer's protocol. Cells were mounted over glass slides using ProLong Gold anti-fade reagent (Molecular probes Inc., USA). The fluorescent images were captured using the DS-Ri2 digital camera (Nikon, Japan) attached to the Nikon Eclipse Ti2 fluorescence microscope (Nikon, Japan).

Immunocytochemical assay

Hei-OC1 cells were cultured on top of poly D-Lysine coated coverslips. After the treatment of rolipram and Kanamycin and Furosemide the cell on the coverslips were fixed using 4% paraformaldehyde for 15mins in room temperature. Next, the cells were permeablized using 100% methanol and incubated in -20^{o} C for 5mins. Following permeablization the cells were blocked in 5% normal horse serum in PBSA (phosphate buffered saline and sodium azide). Then the cells were incubated 2 hours in room temperature with LC3 primary antibody (1:100, Santa cruz) followed by Alexa fluoro 488 anti-mouse secondary antibody (1:300, Molecular probes Inc., USA) and Hoechst (1:1000, Molecular probes Inc., USA) for 1 hour at room temperature. The images were captured using the above mentioned camera attached to the Nikon fluorescent microscope.

Drug induced inhibition of autophagy

To find whether autophagy is the protecting factor against the ototoxic effect I inhibit autophagy activity in the cell by the treatment of Chloroquine. After 24 hours of the subculture I treated rolipram as mentioned above. During the administration of kanamycin and furosemide, chloroquine was added along. Therefore, the lysosomal interaction with the autophagosome is blocked. In this way autophagy was inhibited by drug administration.

***Atg7* knockdown**

I further wanted to confirm this phenomena, so, I knockdown the *Atg7* gene using the *Atg7* siRNA (Bioneer, Republic of Korea). The siRNA was transfected to the cells using lipofectamine RNAimax reagent (Invitrogen, USA). 6 hours after the transfection procedure the media was replaced with medium containing 10% FBS and rolipram was treated at this point of time to the cells. After 48 hours of treatment Kanamycin and furosemide was added together and the cells were kept in incubator for another 24 hours. Protein was isolated and further used for immunoblot analysis.

Immunoblot assay

After the 48hours pre-treatment of rolipram followed by the 24 hours treatment of Kanamycin and furosemide the cells were harvested and total protein was isolated. The harvested cells were washed with phosphate buffered saline and incubated in RIPA buffer (50mM Tris pH7.6, 150mM NaCl, 0.1% SDS, 1.0% NP-40, 1% Sodium deoxycholate, 2mM EDTA) for 30 minutes at 4^{o}C. For the in vivo studies, rat cochlea were homogenized in RIPA buffer using a sterile disposable homogenizer in 4^{o} C. This was followed by centrifugation at 16000g at 4^{o}C for 20mins. The clear lysate contains the total protein and it was collected in a sterile tube. The collected total protein was quantified using Pierce BCA protein assay kit (Invitrogen, USA) and used for SDS-PAGE. After the SDS-PAGE proteins were transferred onto PVDF membranes. The membranes were blocked with 5% normal horse serum in TBS-T (Tris buffered saline and 0.01% Tween-20). The membranes were incubated in 4^{o}C overnight with appropriate primary antibodies Cleaved Caspase 3 (1:200, Millipore, USA), LC3 (1:500, Santa cruz), SQSTM1 (1:700, Santa cruz), GAPDH (1:500, Santa cruz) followed by appropriate horseradish peroxidase conjugated secondary antibodies, Anti-Goat (1:5000), Anti-Rabbit (1:2000), Anti-mouse (1:2000). Blots were developed using Amersham ECL western blotting detection reagents

kit (GE Healthcare, UK) using the manufacturer's protocol. All the captured images were quantified using Image J software (NIH, USA).

Statistical analysis

All the results are expressed in mean and standard deviation. The statistical analysis was performed using Graphpad Prism (v 8. 8.0.1.244). Student's t-test was used to compare two different conditions. P values that are less than 0.05 were considered statistically significant.

3. Results

Kanamycin and furosemide causes Hei-OC1 cell death and rolipram treatment protects the cell death

In order to establish a hearing loss model I used House ear institute – Organ of Corti 1 (Hei-OC1) cells and administered combination of kanamycin and furosemide at different concentration. I have found through MTT cell viability assay that the treatment of 30mM of kanamycin and 3mM of furosemide (Figure 4A, $n = 3$, $p \leq 0.05$) for 24 hours, are the better concentration to induce optimal cell damage required for the study. To determine the optimal concentration of rolipram, I pre-treated the Hei-OC1 cells with rolipram for 48 hours in a dose dependent manner. Pre-treatment of 0.1μM concentration of rolipram gave a significant protective effect in the hair cells (Figure 4B, $n = 3$, $p \leq 0.05$) against the kanamycin and furosemide induced ototoxicity through the MTT cell viability assay. I further wanted to confirm the protective effects by checking the expression of apoptotic marker cleaved caspase 3 through immunoblotting. The immunoblot data (Figure 4C and D $n = 3$, $p \leq 0.05$) showed an increase in the expression of cleaved caspase 3 upon the treatment of K+F and the expression was alleviated when the cells were pre-treated with 0.1μM rolipram. These data shows that the Hei-OC1 cells were protected against the toxic effect of kanamycin and furosemide upon the treatment of rolipram. This opens up the question that how the protective effect is achieved upon the treatment of rolipram.

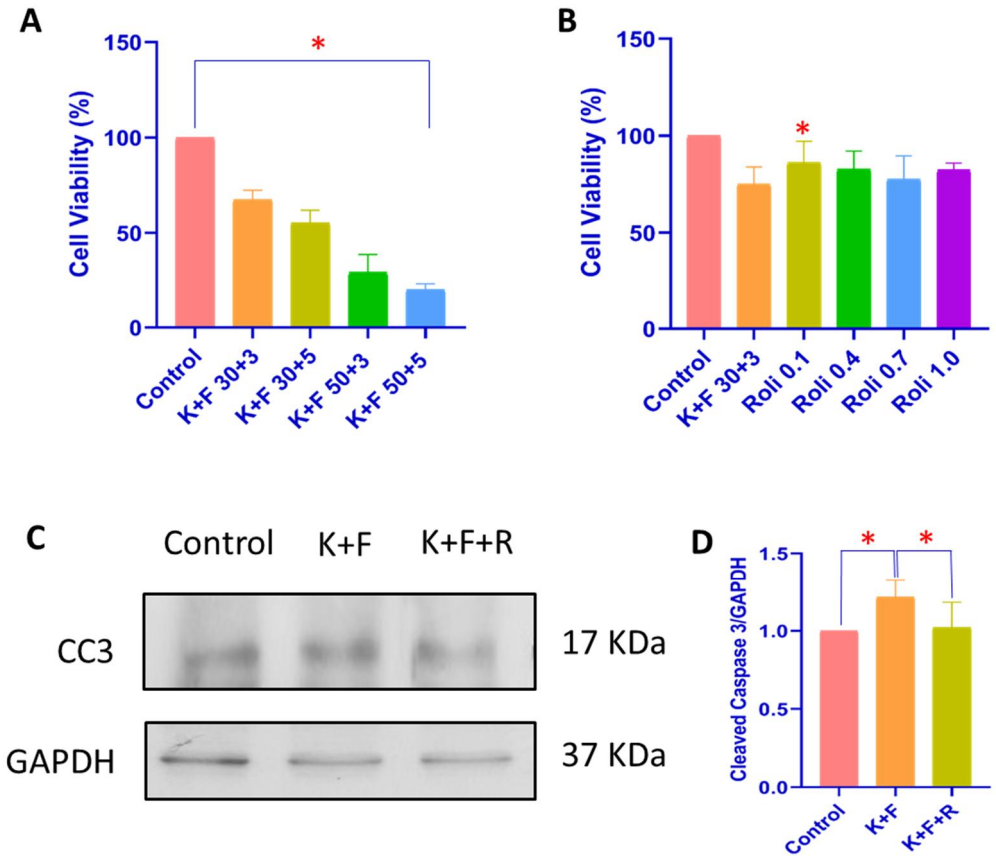

Figure 4. Ototoxic effect of kanamycin and furosemide and the protective effect of rolipram in Hei-OC1 cells**. A)** MTT analysis data shows the dose dependent ototoxicity of kanamycin and furosemide. 30μM and 50 μM of kanamycin and 3μM and 5μM of furosemide concentrations were used. ($n = 3$, $p \leq 0.05$)**. B)** 30μM and 3μM of kanamycin and furosemide were chosen and the resulting MTT data shows the 0.1 μM conc of rolipram was sufficient enough to protect the Hei-OC1 cells against ototoxicity ($n = 3$, $p \leq 0.05$)**. C)** Western blot image shows the expression of cleaved caspase 3. **D)** Cleaved caspase 3 was normalized with GAPDH showing a significant change in the expression of the apotosis marker cleaved caspase3 when compared with control and rolipram treated conditions ($n = 3$, $p \leq 0.05$).

Activation of autophagy upon the treatment of rolipram

As a few studies have already recorded the activation of autophagy in the protection of Hei-OC1 and hair cells during various ototoxic conditions (He et al., 2017). Therefore, I have also wanted to check whether autophagy is responsible for the protective effect on the hair cells upon the treatment of rolipram. I used the CYTO-ID autophagy detection kit to stain the autophagosomes. I used rapamycin as a positive control for the autophagy activity. The results were clear that when compared with the control (Figure 5A i) upon treatment of Rapamycin (Figure 5A ii) and rolipram (Figure 5A iii) I could able to visualize the autophagosome formation. The green fluorescence which depicts the autophagosomes could not be seen in the kanamycin and furosemide treated cells (Figure 5Aiv) and in the rolipram pretreated conditions I could evidently see the appearance of the fluorescence (Figure 5A v). This denotes the failure of the cells to produce the autophagosomes. This was later confirmed by immunocytochemical staining with the LC3 antibody (Figure 5B). In the rolipram treated condition, formation of the LC3II puncta can be clearly seen increased when compared with the control and the untreated conditions (Figure 2B). The formation of LC3 puncta confirms the conversion of the LC3I into LC3II.

The immunoblotting data also shows an increase in the LC3II level in the rolipram treated condition when compared to the untreated condition and no expression can be seen in the control (Figure 5 C and D $n = 3$, $*p \leq 0.05$, $**p \leq 0.01$). The absence of the LC3II in the control can be due to the fact that the cells are not under any stressful condition (free from kanamycin and furosemide). Autophagy is a stress responding mechanism, therefore upon the treatment of kanamycin and furosemide the stress induces the activation of autophagy. As earlier mentioned studies shows the failure of the autophagy flux upon ototoxic conditions, I have checked the expression level of SQSTM1. SQSTM1 is ubiquitin protein that recruits the damaged proteins and organelles into the

autophagosomes. This was then degraded by lysosome. Therefore during the failure of autophagy flux there won't be any degradation process. So the level of SQSTM1 will be higher. This phenomena can be seen in Figure 5E and Figure 5F ($n = 3$, $p \leq 0.05$). The expression level of SQSTM1 was higher in the kanamycin and furosemide treated condition when compared with the control and rolipram treated condition. In fact the expression level in the rolipram treated condition was significantly reduced depicting that the autophagy flux is being restored upon the treatment of rolipram. From these results I could say that the autophagy has been activated during the stress condition but the autophagy flux has been damaged upon toxic condition. Rolipram treatment restores the impaired autophagy flux. But I need further evidences to confirm that autophagy is the real protector of the Hei-OC1 cells.

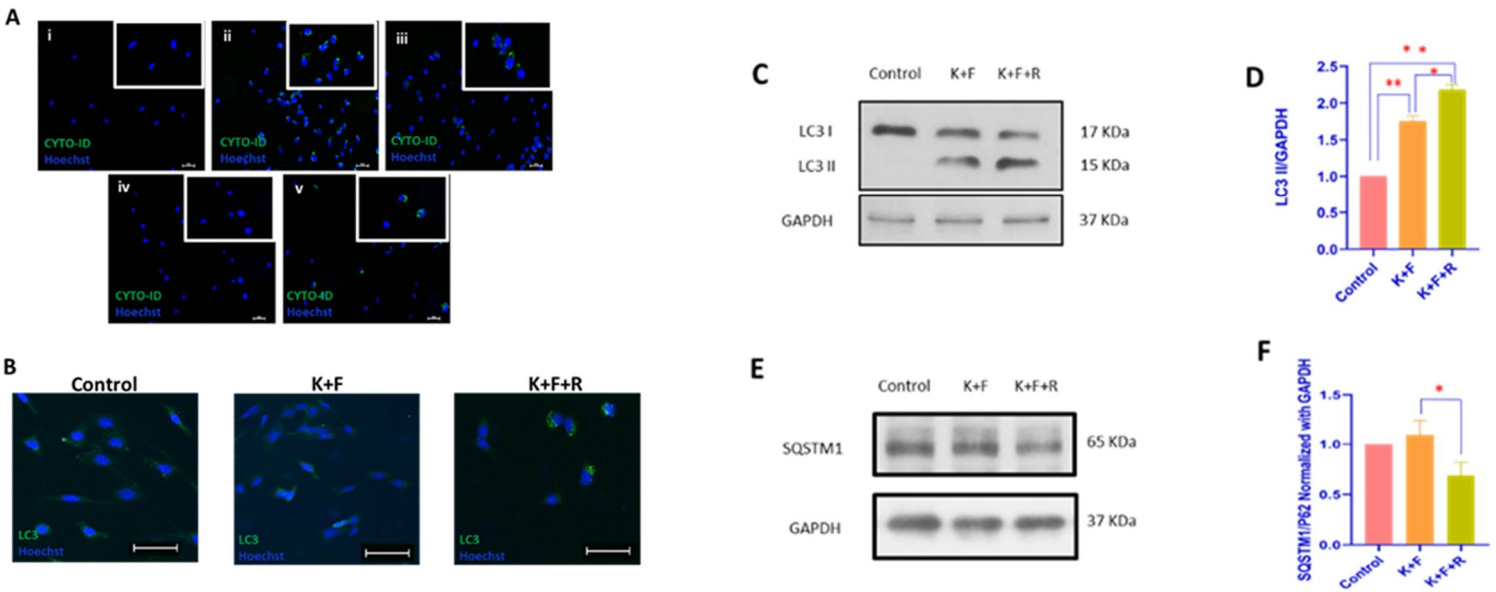

Figure 5. Higher activity of autophagy upon rolipram treatment. **A)** The CYTO-ID staining of the Hei-OC1 cells **(i)**Control, **(ii)** Rapamycin positive control **(iii)** Rolipram, **(iv)** Kanamycin and furosemide, **(v)** Rolipram treated along with K+F. **B)** Immunocytochemical staining shows the formation of Autophagy puncta upon the treatement of rolipram. **C)** Western blot image showing the expression of LC3 I and II. **D)** LC3 II expression was normalized with GAPDH showing a significant increase in the expression of LC3 II when compared with the control ($n = 3$, * $p \leq 0.05$, ** $p \leq 0.01$). E) western blot showing the expression of SQSTM1. **F)** Graph showing the significant differences in the expression of SQSTM1 between rolipram treated and untreated conditions ($n = 3$, $p \leq 0.05$)**.**

Inhibition of autophagy could not prevent the Hei-OC1 against kanamycin and furosemide

I designed two strategies to confirm that the protective effects is because of the autophagy activation. One strategy is to use an autophagy inhibitor and the other is the use of siRNA to knockdown the autophagy mechanism. After pre-treating the Hei-OC1 cells with 0.5μM of rolipram for 48 hours, the cells were treated with 30μM of chloroquine along with kanamycin and furosemide for the next 24 hours. Therefore the autophagy flux will be blocked. This is because chloroquine inhibits the interaction between lysosome and the autophagosome membrane. Therefore the lysosomal degradation of the autophagosomes will be stopped. This was evidently seen from Figure 3A that the choloroquine treated conditions show an increased expression of LC3 II. Upon observing the chloroquine induced autophagy inhibition experiment results it is evident that the LC3 II level in the rolipram treated cells was significantly higher (Figure 6B $n = 3$, $p \leq 0.05$) when compared to cells which have not been treated with Chloroquine, denoting the block of autophagy flux. This can also be seen in the expression of SQSTM1 levels (Figure 6A, 3C, $n = 4$, $p \leq 0.05$). The chloroquine treated cells shows a significant increase in the expression of SQSTM1 when compared with the chloroquine untreated condition (Figure 6C $n = 4$, $p \leq 0.05$). As I have impaired the autophagy flux by using chloroquine I checked the expression levels of the apoptosis marker cleaved caspase3. As expected the expression level of cleaved caspase 3 was significantly increased (Figure 6D, $n = 3$, $p \leq 0.05$) in the chloroquine treated condition. The results of this experiment clarifies that blocking the autophagy flux could results in cell death and restoring it results in the protection of the Hei-OC1 cells.

I further wanted to confirm this by inhibiting the autophagy mechanism by using the siRNA form *Atg7* gene. *Atg7* promotes the conversion of LC3I into LC3II, which was recruited to the phagophore membrane and helps in the elongation and the formation of

autophagosome. The optimization of siRNA was performed and I chose 30μM siRNA (Figure 7 A, B and C). From Figure 6 E and F ($n = 3$, $p \leq 0.05$) I could see that the level of LC3II was significantly decreased in the siRNA treated cells when compared to the negative control. Later the protective effect can be seen by the expression of cleaved caspase 3 (Figure 6G and 6H, $n = 3$, $p \leq 0.05$). Though rolipram was treated in the siRNA condition the expression of cleaved caspase 3 was significantly higher when compared with the negative control treated condition and also the untreated condition. From these data I could clearly say that rolipram's protective effect in the Hei-OC1 cells upon the treatment of kanamycin and furosemide is by the restoration of the autophagy flux by enhancing the autophagy activity and also the lysosomal degradation.

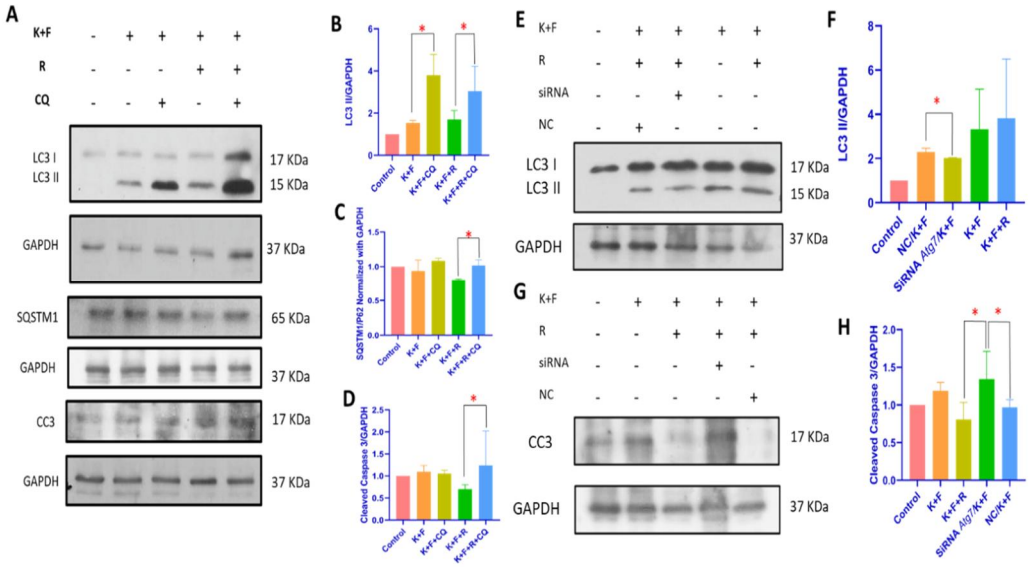

Figure 6. Rolipram could not protect the Hei-OC1 cells against the ototoxicity upon inhibition of autophagy. **A)** Immunoblot of expression levels of LC3, SQSTM1 and Cleaved Caspase 3 upon the treatment of Chloroquine. **B)** Graph showing the significant increase in the LC3 2 expression level upon the treatment of chloroquine ($n = 3$, $p \leq 0.05$). **C)** The expression level of SQSTM1 was significantly increased in the chloroquine treated condition when compared with the rolipram treated condition ($n = 4$, $p \leq 0.05$). **D)** Expression of cleaved caspase 3 is also increased significantly upon the inhibition of autophagy by chloroquine when compared with the only rolipram treated condition ($n = 3$, $p \leq 0.05$)**.** E & G) western blot image shows the expression of LC3 and cleaved caspase 3 respectively. **F)** Graph showing the significant difference in the expression of LC3II between the autophagy knockdown and Negative control (NC) conditions ($n = 3$, $p \leq 0.05$) **G)** Graph showing the significant difference in the expression levels of cleaved caspase3 between autophagy knockdown condition, negative control and rolipram treated conditions ($n = 4$, $p \leq 0.05$)**.**

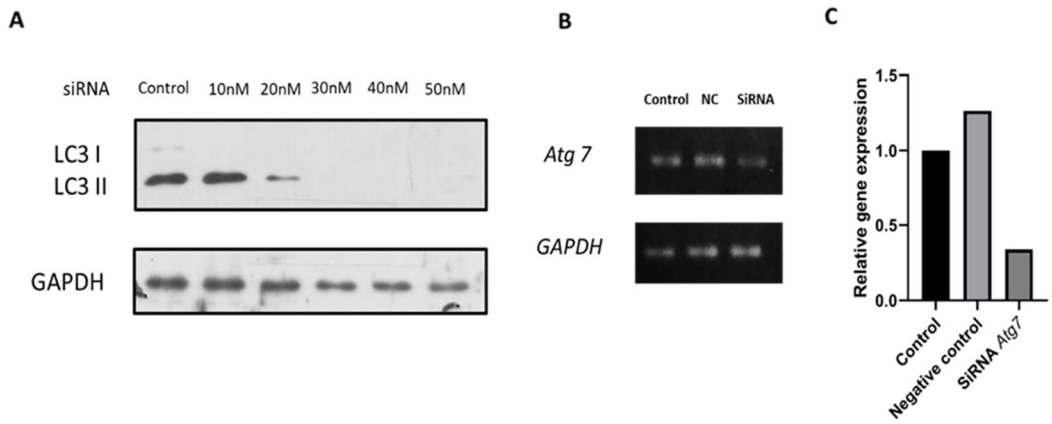

Figure 7. The selection of the concentration of the siRNA to inhibit the autophagy process. **A)** Immunoblot of the expression levels of LC3 upon different concentration of *Atg7* siRNA **B)** Agarose gel electrophoresis after PCR on samples to verify the inhibitory activity of siRNA when compared to control and a negative control (NC) or scramble. **C)** Relative gene expression of *ATG7* in control, negative control and siRNA treated cells.

4. Discussion

Sensorineural hearing loss is a major problem which affects people of all ages. Apart from aging the sensorineural hearing loss is also caused by various other modes like loud noises and intake of ototoxic drugs. It is a result of loss of either inner or outer hair cells or both. This causes the degeneration of SGN. Though there are various strategies like hearing aid or cochlear implants are available, it is necessary to stop the SGN degeneration for a permanent remedy (Nadol et al., 1989). Various recent studies have shown that the activation of autophagy protects the sensorineural hair cells from oxidative stress induced ototoxcity (Fu & Chai, 2019; Ye et al., 2018). Therefore I wanted to adopt this strategy to prevent the Hei-OC1 cells from the cytotoxicity induced by Kanamycin and furosemide.

Autophagy is a catabolic process that recycles the unwanted and toxic substances from the cell's surface. Upon evolution it has been evolved as a cell survival mechanism (Vijayakumar & Cho, 2019). From my previous unpublished study I observed the activation of autophagy by rolipram in the rat fetal neural stem cells. Therefore I used rolipram to activate autophagy to prevent Hei-OC1 cells from the cytotoxicity induced by kanamycin and furosemide. As expected the treatment of kanamycin and furosemide was toxic to the cells. Cells cytotoxicity was reduced after during the treatment of rolipram. This was confirmed by the increase in the cell viability and also the decreased expression of apoptosis marker cleaved caspase 3 (Figure 4 C and D). Next I checked the role of autophagy in this protective effect. I used three different techniques to visualize the autophagy activity. The CYTO-ID staining and the immunocytochemical staining with the LC3 antibody shows confirms the formation of autophagosomes in the rolipram treated cells (Figure 5A and B). Similar to the previous studies it is the kanamycin and furosemide treatment activates the autophagy mechanism as a stress response. This could be said because the conversion of LC3I to LC3II was also observed in the rolipram untreated condition (Figure 5C). But the expression level was less when compared with

the rolipram treated condition. As autophagy is a stress response mechanism, the accumulation of cAMP upon the treatment of rolipram activates ERK pathway (Ugland et al., 2011) which in turn enriches the autophagy during the stress induced by kanamycin and furosemide. Though I could see the expression of LC3 II in the kanamycin and furosemide treated condition, the cells were not protected. This might be because of the failure of autophagy flux and it has also been reported previously (Ye et al., 2019). So to check the completion of autophagy flux I checked for the degradation of SQSTM1/P62. SQSTM1/P62 is an autophagosome cargo protein that recruits the unwanted cargo to the autophagosome for degradation (Bjørkøy et al., 2005; Puissant et al., 2012). Therefore, upon the failure of autophagy flux SQSTM1/P62 will be accumulated in the cell. I found out that the expression of SQSTM1/P62 was decreased in the rolipram treated cells, meaning that the degradation was happening and the increased SQSTM1/P62 level indicated an accumulation of the protein due to the failure of autophagy flux (Figure 5E and F). With this result I confirm that the treatment of rolipram supports the completion of autophagy flux.

It is now known that the autophagy flux is an important step in the protection of hair cell loss. In this study I have added more evidences on the role of autophagy flux in the protection of sensorineural hair cells and prevention from hearing loss. I rather confirmed this phenomenon by blocking the formation of autolysosome (the fusion of autophagosome and lysosome), by using chloroquine. The theory behind this is that, when chloroquine is treated the lysosomal fusion with the autophagosome was blocked (Mauthe et al., 2018). Therefore the degradation step will not occur and as a result the autophagosome start to accumulate on the cell surface. The results from chloroquine induced autophagy flux inhibition shows, there was an accumulation of LC3 II and SQSTM1/P62 (Figure 6A, B and C) and rolipram failed to protect the Hei-OC1 cells upon the treatment of cholorquine. Proving the importance of the completion of autophagy flux

to attain protection against cytotoxicity. I also knocked down the *Atg7* gene, which prevents the formation of LC3II and inhibits the autophagy progression (Frudd et al., 2018). The knock down results were also similar, i.e., rolipram treatment could not protect the cells upon cytotoxic condition. Though autophagy was activated when kanamycin and furosemide was treated as a stress response, the formation of autolysosome was not occurred. Therefore the degradation have not ensued. From my results it is evident that rolipram enriches the autophagy flux and clears the cytotoxic agents and protects the Hei-OC1 cells from kanamycin and furosemide. As this is a model for hearing loss I could say that the pharmacological interventions which targets to enhance the autophagy flux could be a better strategy in treating sensorineural hearing loss patients.

III. PART 2. DNA Methylation Aging Clock

Chapter 1

Pan-Tissue Methylation Aging Clock: Recalibrated And A Method To Analyze And Interpret The Selected Features

1. Introduction

The recent development of the array technology introduced more target CpG sites and the latest addition to the illumina array is the EPIC methylation array beadchip which covers over 850K CpG sites. In my study, I wanted to include a broad range of DNA methylation sites. I assumed, this inclusiveness could cover more DNA regions, which may involve in the aging process and results in identifying more important methylation sites during the feature selection. Recently deep learning models have been showing promising performance in various fields, implying that technology in age prediction will yield a better predictive accuracy. Deep learning derived clock model has also been recently published (F. Galkin et al., 2021).

In the present study, I explored the potential of the advancement in the array technology to develop a DNA methylation clock that could predict the age of different tissues. In the process, I have developed a model with a higher accuracy and lesser error in the test data when compared with the already existing multi tissue clocks. In addition, this model have performed better in predicting the age of the tissues, which have not been used in the training session. Further, I have also analyzed the probes selected by the machine learning model to find out the biological meaning behind these DNA methylation age probes as they undeniably capture the essential characteristics of aging epigenome (Horvath & Raj, 2018).

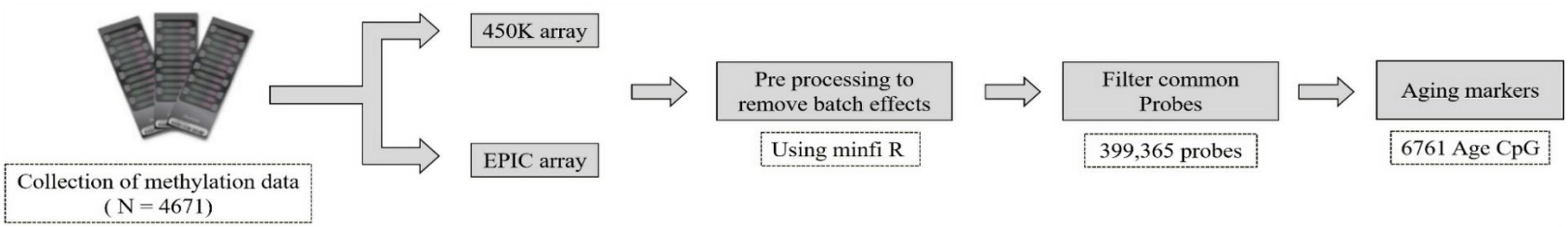

Figure 8. A graphical representation of the study flow. Various datasets of different tissues were collected. The data were preprocessed and common probes where filtered. Once the data were organized for machine to be read the training session begins.

2. Methods

Dataset collection

All the datasets used in this study have been collected from the public database Gene Expression Omnibus. In Figure 8 the study process have been graphically explained. If the original study of the datasets includes any disease samples, they were neglected and only the control samples from the datasets has been used. Therefore, all the data used in this study were of normal humans. I used 20 different tissues datasets, which comprises 4671 samples for the training and test. The list of datasets used for training and test are given in Table 2. All the datasets collected were obtained from different tissues on either Infinium Human Methylation 450k or EPIC 850k methylation array platform. Only the study with the availability of the person's age and IDAT format raw files were collected, so that all the datasets will be preprocessed with the same preprocessing technique. The data consisted of samples with ages ranging from 0 to 103 in the training set and 0 to 102 in the test dataset. Table 2 shows the details of the datasets used and the spread of age range throughout the dataset. I made sure that the age range spread in both the training and the test data are similar. Equal age distribution have been ensured in all the quartile of the datasets (Table 3). It has been already known that increasing the age range and similar age distribution in training and test data will improve the accuracy in prediction(Qian Zhang et al., 2019).

Preprocessing of the data

The 'minfi' R package was used for the normalization of the batch effects and the calculation of the beta values from the RAW files (Aryee et al., 2014; Fortin et al., 2017; Touleimat & Tost, 2012). By using the preprocess quantile, the data were normalized and the beta values were obtained. The quantile normalization performs both normalization and also corrects the shifts in the infinium I and the infinium II probes. Due to the data

availability, I finalized to use the common probes between the 450K methylation array and the 850K array. Only 399,365 common CpG probes between the 450k and the EPIC array were used which does not include the sex chromosome sites. I used umbilical cord blood samples as Zero age.

Machine learning

Elastic net regression algorithm was used for generating this methylation age prediction model as it can be used for feature selection. Python 3.6 has been used as a programming platform. sklearn packages were used to compile the elastic net regression. Hyper parameter tuning was performed using the sklearn.gridsearch package with 10 fold cross validation. The 10 fold cross validation ensures the robustness of the model after numerous repeating of the training session. The best-fit value of l1 ratio and alpha value were 0.5 and 0.1 respectively. These were used for the model establishment. The whole data were split for training and test using the sklearn train_test_split. 1/3rd of the total data was used as test data. Therefore the training and test set consisted of 3114 and 1557 samples respectively. Once the training session has ended, the model selected 6761 probes. Recursive feature elimination was performed by the sklearn package for feature selection using the linear kernel.

Pathway enrichment

Pathway enrichment analysis was performed by the G:Profiler online software (Raudvere et al., 2019). Gene ontology terms for molecular functions, Cellular components and Biological processes were used. The significance threshold was controlled by using Bonferroni correction with a p value ≤ 0.01. To make the GO bar diagram which shows the number of genes involved in the enrichment of a single pathway I used web based gene set analysis toolkit (Liao et al., 2019).

Statistical analysis and data visualization

The accuracy metrics MAE, RMSE and the R^2 were determined using the sklearn.metrics (v.0.24.2) (https://scikit-learn.org) in Python 3.8. Heat map was generated with Seaborn (v.0.11.2) for python. The Venn diagram was made using the matlplotlib Venn for python. All the data visualization was done with GraphPad Prism Version 8.0.1.

Table 2: Details of the datasets used for the study.

S.NO	GEO ID	Tissue	No of Samples
1	GSE147740	Peripheral blood (mononuclear cells)	1032
2	GSE87571	Whole blood	729
3	GSE74193	Prefrontal cortex	418
4	GSE88883	Breast tissue	100
5	GSE134379	Middle temporal gyrus	173
6	GSE134379	Cerebellum	177
7	GSE119078	Saliva	59
8	GSE132547	Broncho alveolar lavage fluid	24
9	GSE137716	Bronchial brush	16
10	GSE151042	Umbilical cord blood	454
11	GSE90060	Uterine Endometrium	32
12	GSE59065	CD8+ T cells	96
13	GSE59065	CD4+ T cells	95
14	GSE129428	Hippocampus	32
15	GSE157341	Liver	35
16	GSE107038	Liver	40
17	GSE125895	Dorsolateral prefrontal cortex,	196
18	GSE125895	Hippo, Cerebellum, entorhinal cortex	
19	GSE154566	Buccal swab	900
20	GSE79100	Human Kidney	31
21	GSE138307	Bone	32
		Total samples	**4671**

Table 3: Showing the details of datasets used in the study.

Dataset	N	Mean age	1st Quartile	Median age	3rd Quartile	Age range
Training	3114	36.5	18	36	53	0-103
Test	1557	36.9	18	36	54	0-102

3. Results

Performance of the model in Training and test data

To verify the model's performance, I used various metrics like Root Mean Squared Error (RMSE), Mean Absolute Error (MAE) and the correlation coefficient R^2 values, which were measured between the actual age and the predicted age (Figure 9A and C). The R^2 value explains the proportion of the variance. RMSE and MAE were used to measure the average error in the prediction. Table 4 shows the performance values of the clock model in both test and training set data. The R^2 value for the training data was 0.99 and the test was 0.97. I observed a MAE of 1.62 years in the training data and a MAE of 2.8 in the test data. RMSE for the training set data is 2.3 years and RMSE for the test set data is 4.4 years. These statistical numbers shows that the methylation clock is almost accurate in the training data and equally good when applied to an unknown data also. The residual plot shows a random pattern suggesting that the model is a good fit in both the training and the test datasets (Figure 9B and D).

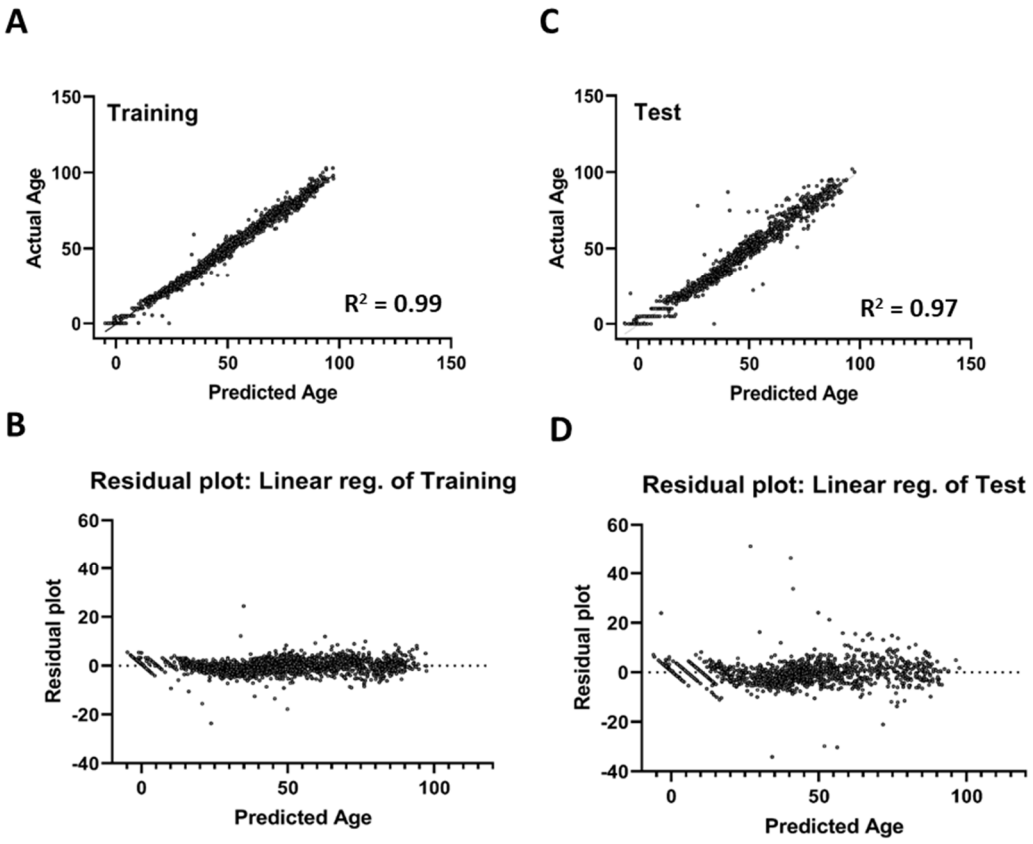

Figure 9. Performance of the model on both training and test data. A and C) Correlation between actual age and the predicted age of the training set (MAE=1.6 years) and test set data (MAE=2.8 years) respectively, B and D) Residual plot of the training data shows a normal pattern, denoting the model is trustworthy.

Table 4: Showing the accuracy metrics of the model.

Dataset	Correlation(R^2)	RMSE	MAE
Training	0.99	2.3 years	1.62 Years
Test	0.97	4.4 years	2.8 Years

Performance of the model in different tissues:

To validate how this pan-tissue model is working in different tissues, I tested the model over each individual tissue data sets, which I used for training and test. The accuracy in most of the tissues, which have been used in the training data, are good (Figures 10A-O). Among the tissues used in the training data only the bone tissue shows a below average prediction accuracy. The R^2 value and the other metrics were also better in almost all the tissues, which were used for training the model (Table 5). I also tested the model on tissues and cell types, which were not used in the training session, to verify the model's performance (Figures 11A-E). The accession ids used for the verification are as follows: GSE151732 (Devall et al., 2020), GSE164195 (Pepin et al., 2021), GSE173356 (Konigsberg et al., 2021), GSE66351 (Gasparoni et al., 2018). Except for the heart tissues, the accuracy of age prediction in these validation tissues data was moderately good showing a better RMSE between 4 years to 9 years and a MAE between 3.9 to 7.8 years (Table 6).

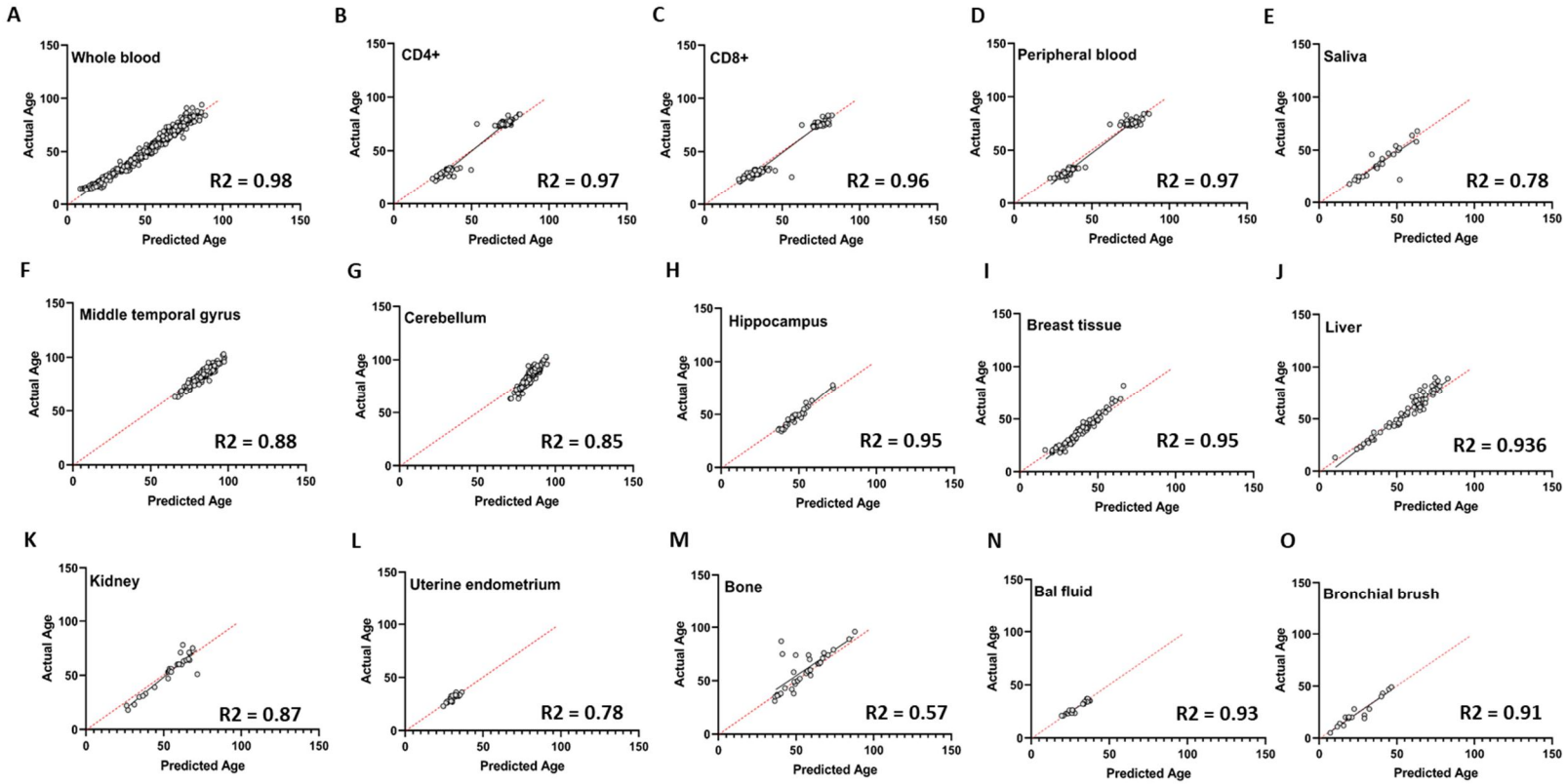

Figure 10. Performance of the methylation clock on various different tissues. Red dotted line denotes the regression line of the training dataset.

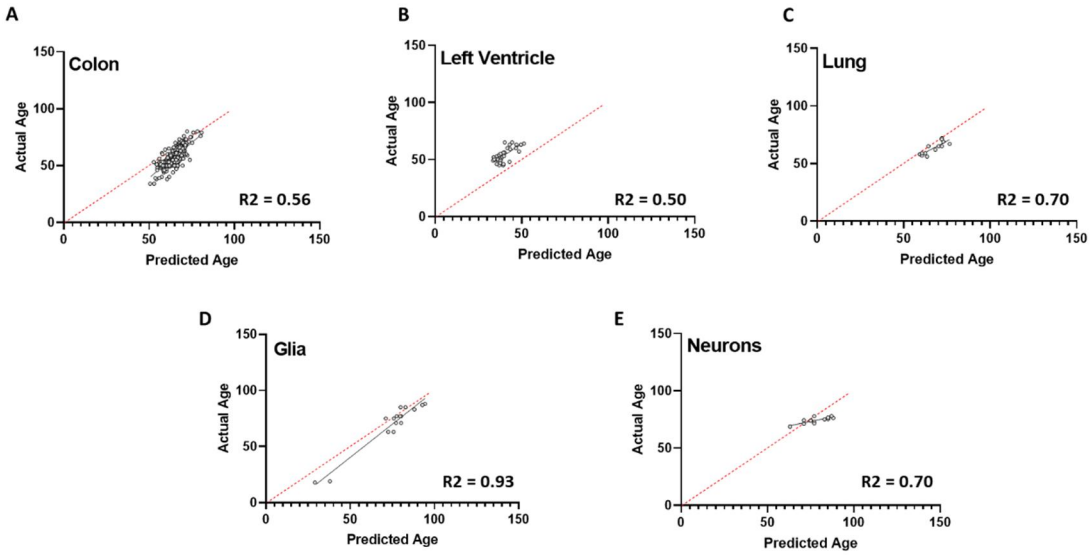

Figure 11. Performance of the methylation clock on various different tissues, which have not used in the training data. Red dotted line denotes the regression line of the training dataset.

Table 5: Accuracy metrics of the model in various tissues.

Tissue	Correlation(R^2)	RMSE	MAE
Whole blood	0.98	2.66 years	1.98 years
CD4+	0.97	5.1 years	4.01 years
CD8+	0.96	4.96 years	3.37 years
Peripheral blood	0.97	4.74 years	3.83 years
Saliva	0.78	6.63 years	3.72 years
Middle temporal gyrus	0.88	2.75 years	2.22 years
Cerebellum	0.85	4.06 years	3.15 years
Hippocampus	0.95	2.95 years	2.37 years
Breast Tissue	0.95	3.75 years	2.87 years
Liver	0.93	5.79 years	4.40 years
Kidney	0.87	6.40 years	4.32 years
Uterine endometrium	0.78	1.53 years	1.19 years
Bone	0.57	12.23 years	6.87 years
BAL fluid	0.93	1.52 years	1.15 years
Bronchial brush	0.91	3.81 years	2.79 years

Table 6: Accuracy metrics of the model in various tissues that are not used in the training session.

Tissue	**Correlation(R^2)**	**RMSE**	**MAE**
Colon	0.56	9.22 years	7.87 years
Heart	0.50	14.01 years	14.68 years
Lung	0.70	4.86 years	3.91 years
Glia	0.93	7.98 years	6.46 years
Neurons	0.70	6.36 years	5.27 years

Change of trend in the methylation pattern:

The selected 6761 probes have been considered as aging probes. To check the methylation pattern of the selected probes upon aging, I generated a heat map with the beta values of each probes (Figure 12A). I calculated the average of each probe's beta value on every age starting from 0 to 103. Considering age 25 as the mid-point, the data were arranged from hyper to hypo methylation. I considered 25 years of age as the phase from which the aging begins, as previous studies have also considered this as an early adult phase (Caplan, 2007). This could be also seen in Horvath clock's ticking rate (Horvath, 2013), where he explains that a high ticking rate could be seen during an organismal growth and it gets slower and a constant change could be seen after adulthood. Upon observing the heat map (Figure 12A), the change in each individual probe level was minute and a similar pattern was observed in the Horvath's clock. The machine learning models predicts the dependent variable by the collective added weights of all the selected probes. Therefore, I took the average of the beta values of all the 6761 probes of each age and checked for the collective change in the pattern of methylation of these age probes. The Weighted average change in the young and adolescent age was not constant. It showed a noisy uneven change (Figure 12B). This could be due to the developmental changes, which have been interfering. After the early adult age around 35 years, there is an increase in the collective average of the methylation and this continuous increase gradually slows around the age of 80 years (Figure 12B). This shows that the aging process in fact have an impact in the aging methylation sites.

I segregated the probes into two groups by performing a multiple linear regression with all the selected 6,761 age probes. I highly scrutinized the probes using their p values. One group of probes with p value ≤ 0.0001 comprised of 3659 probes and other groups, which had higher p values comprising 3102 probes. When the trend in the methylation of these probes with lesser p values were analyzed, most of these CpGs are highly

hypermethylated and a few are hypomethylated (Figure 13A and B). Stating that DNA methylation pattern is altered upon aging process.

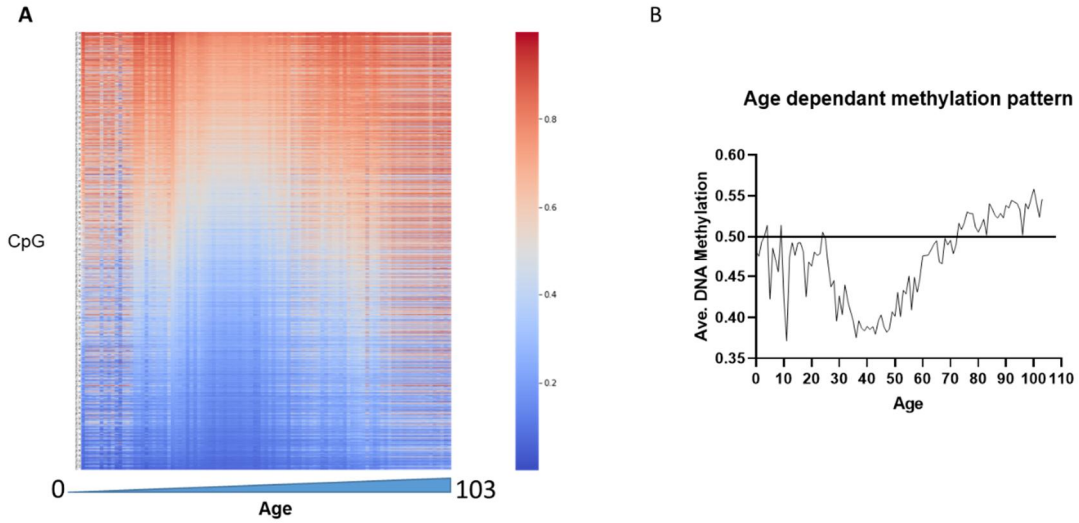

Figure 12. Change in the methylation pattern of the selected probes. A) Heat map showing the methylation levels of all the selected probes. B) Weighted average DNA methylation change from 0 – 103 years.

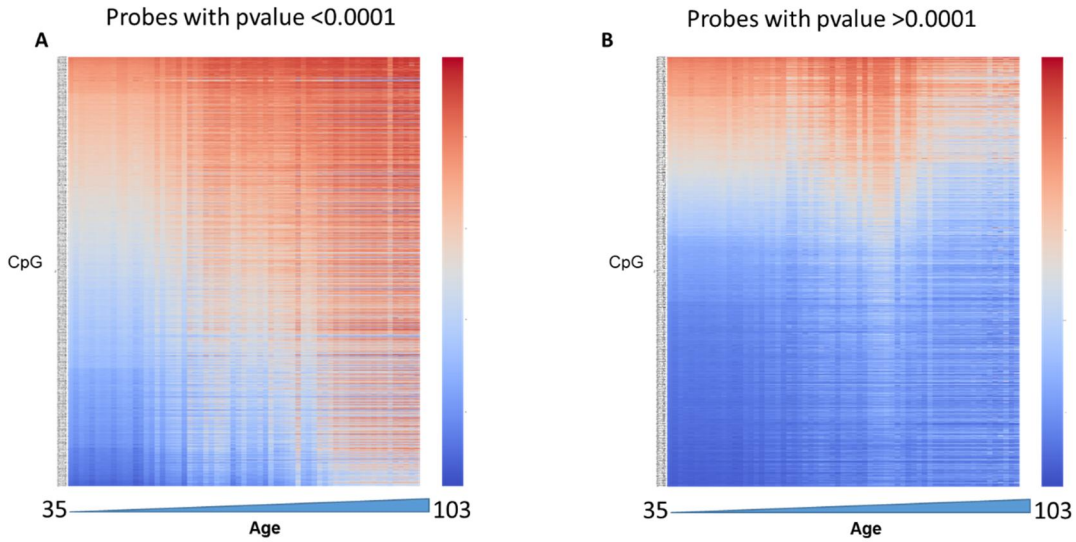

Figure 13. Selected CpG probes have been separated according to their p values. **A)** Heat map showing the CpG probes with pvalue ≤ 0.0001 **B)** Heat map showing the CpG probes with pvalue > 0.0001

Pathway Enrichment Analysis:

The 6,761 selected age probes were annotated with their respective gene ids using the Illumina 450k annotation. It resulted in 4,120 genes. By using these genes, I checked for the enriched pathways. The highly enriched gene ontology terms were anatomical structure development, multicellular organism development, nervous system development, developmental process, system development, multicellular organismal process, behavior, central nervous system development, cell morphogenesis, cell development, neurogenesis, anatomical structure morphogenesis, animal organ development, brain development, head development, generation of neurons and cell morphogenesis involved in differentiation (Figure 14A). 1588 genes were annotated for the Gene ontology described pathways. Most of the enriched pathways were of early development related pathways like, 886 involved in biological regulation, 537 in Developmental process, 101 in reproduction, 805 in Metabolic process and many others (Figure 14B). These pathways can be classified into Energy metabolism related pathways (biological regulation, metabolic process), Stress maintenance (response to stimulus and cell communication) and Growth and development (multicellular organismal process, developmental process, cell component organization, cell proliferation, reproduction and growth). Upon searching to find an answer to address why the development related pathways have been enriched, in the deepMage study (Fedor Galkin et al., 2021), the authors of the study have addressed this by relating it with the antagonistic pleiotropy theory (Fedor Galkin et al., 2021; Williams, 1957). According to the antagonistic pleotropic theory of aging some genes controls several other traits and regulate them in positive manner in early stage and regulate those oppositely in the later stages of the life resulting in the various after-effects of aging process (Williams, 1957). Exploring these genes further will shed light on how these genes interact and take part in the aging process collectively.

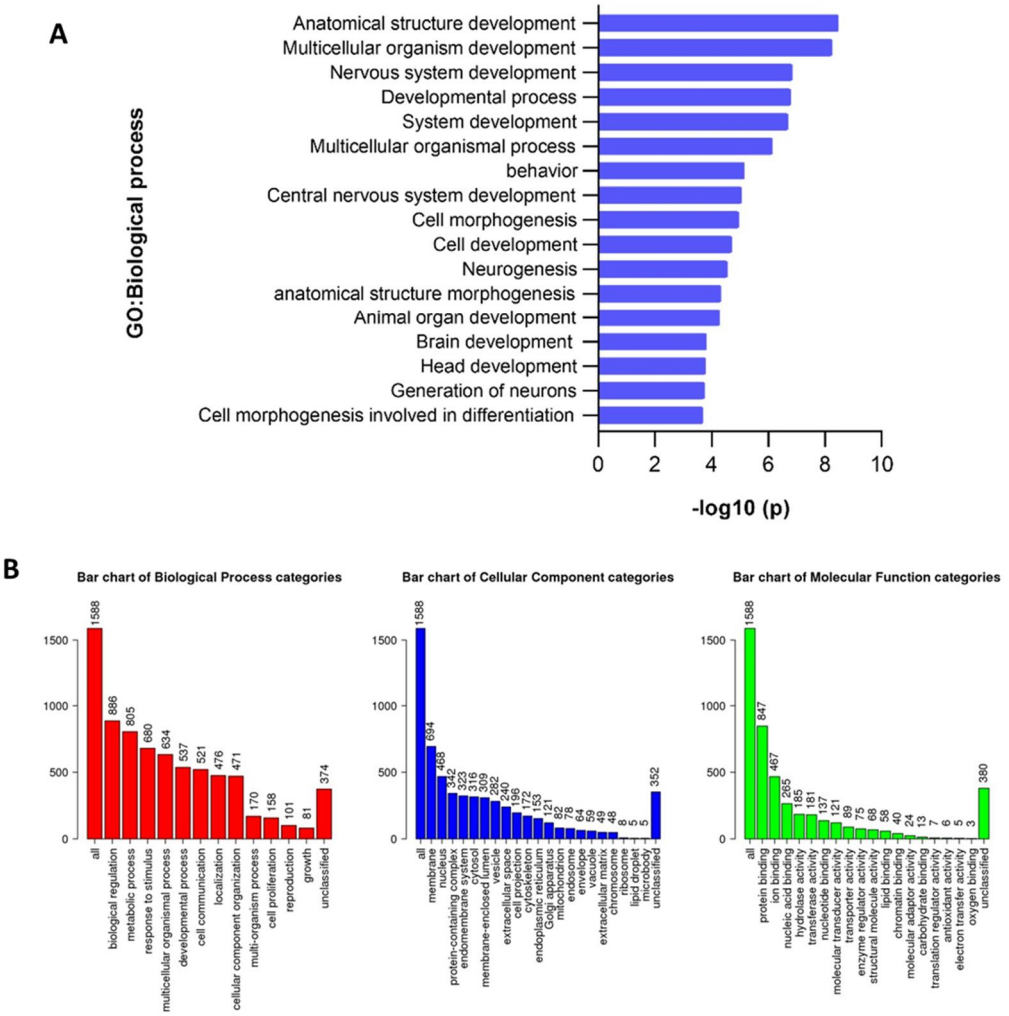

Figure 14. Pathway Enrichment analysis. A) Pathway enrichment of gene ontlology terms for biological process showing the highly enriched pathways. B) Showing number of genes in each enriched pathways according to the Gene ontology.

Comparing the Selected Age probes with known aging related genes:

First, I have compared the selected probes of my clock model with Horvath's model to know how many probes are shared between both the models. 334 probes have been shared between both the models. In order to know how many of the annotated genes of my probes have been reported already, I curated genes from two databases, namely GenAge and CellAge (Avelar et al., 2020; de Magalhães & Toussaint, 2004). Both these databases belong to the Human Aging Genomic Researches database. GenAge is a collection of Human genes, which are involved, in the aging process and CellAge is a database, which consist of human senescence associated genes that have been curated from various gene manipulation experiments and gene expression profiling. As my DNA methylation clock is human based I curated only genes, which are related to human aging, therefore I choose these two databases. The total number of genes curated from these databases yielded 554 genes. Among them 97 genes are common from my model-selected ones. Between them 48 genes were mutual between my age probes and the GenAge genes and 56 were common genes with CellAge database (Figure 15 A and B) (Table 7). Then I checked for how many of those genes were shared between the multiple linear regression wise separated genes with p value ≤ 0.0001. I found out that 62 genes out of the 97 known genes were common between the probes, which had p value ≤ 0.0001 (Figure 15C and D). These 62 genes corresponds to 80 CpG probes (Table 8), the methylation pattern of these probes were highly hypermethylation, and a few are hypomethylated (Figure 15E). Among the 62 genes, many of the commonly used aging related markers like TP73, FOXO1, mTOR and inflammatory markers like TNF, STAT3, STAT5A and CDK can be found (Table 8). Next, I performed pathway enrichment analysis with these common known genes to find the enriched pathways. The top 10 highly enriched gene ontology terms for biological process are regulation of cell death, negative regulation of cell death, regulation of programmed cell death, negative regulation of apoptotic process, cell death, regulation of apoptotic process, negative regulation of programmed cell death, response

to hormone and regulation of cell population proliferation (Figure 15F). Without a surprise, most of the enriched pathways are negative regulation of apoptosis, cell proliferation, regulation of cell death and response to hormone. The negative regulation of apoptosis and regulation of cell proliferation denotes the process of cells going into senescent state as it is Well known that senescent cells show resistant toward apoptosis (Jeong & Cho, 2016; Soto-Gamez et al., 2019). All of the pathways that are enriched can be considered as mechanisms, which are all the consequences of the aging process.

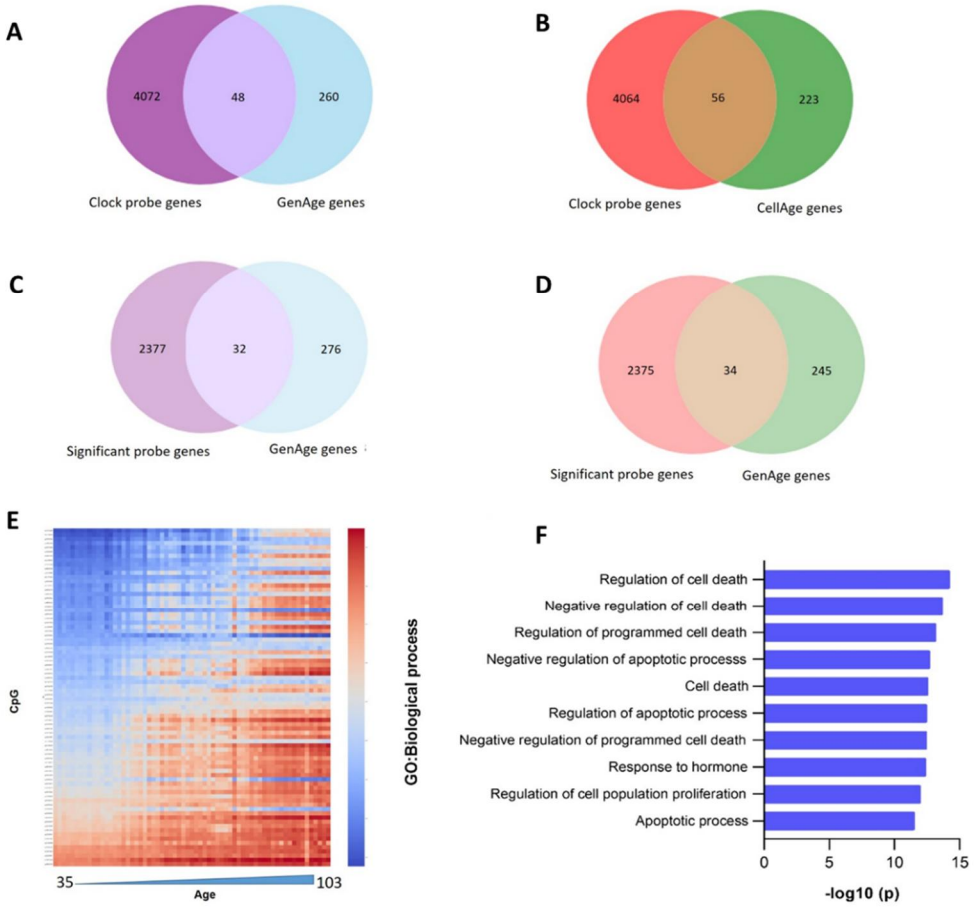

Figure 15. Comparison with known genes curated from different databases. A and B) Common genes with the methylation age probes. C and D) Common genes between the highly significant probes ($p \leq 0.0001$) has been shown in the Venn diagrams. E) Heat map showing the change in the methylation pattern of highly significant probes which falls over the common known genes. F) Pathway enrichment of the genes which are common between the highly significant probes and known aging related genes.

Table 7: Showing the list of known aging related genes from GenAge and CellAge

S.No	GenAge Genes	Cell Age genes
1	ADCY5	AAK1
2	BCL2	ATF7IP
3	CAT	BAG3
4	CDK1	BCL6
5	CDKN1A	BHLHE40
6	CETP	BLVRA
7	CSNK1E	CAV1
8	CTNNB1	CBX7
9	DLL3	CCND1
10	EGF	CDK1
11	EIF5A2	CDK18
12	ERBB2	CDKN1A
13	ERCC1	CDKN1B
14	ERCC2	CDKN1C
15	ESR1	CKB
16	FOXO1	DDB2
17	GSTP1	DUSP3
18	HDAC1	ETS2
19	HOXC4	EWSR1
20	HSPA1B	FXR1
21	IGF1R	GATA4
22	IL7	GNG11
23	JAK2	GRK6
24	KCNA3	HDAC1
25	LMNA	HDAC4
26	MAP3K5	HEPACAM
27	MAX	IGFBP1
28	MSRA	IRF7
29	MTOR	KCNJ12
30	MXI1	KDM4A

Table 7: Continued

S.No	GenAge Genes	Cell Age genes
31	NCOR2	MAP3K6
32	NFE2L2	MMP9
33	PAPPA	MYLK
34	POLG	NDRG1
35	PRKCA	NFE2L2
36	PTK2B	NINJ1
37	SOD2	OTX2
38	SP1	PAK4
40	STAT3	PKM
41	STAT5A	PRKCH
42	SUN1	PTRF
43	TERT	RUNX1
44	TFAP2A	SENP2
45	TNF	SGK1
46	TOP2B	SIX1
47	TP63	SLC16A7
48	TP73	SP1
49	-	STK32C
50	-	STK40
51	-	SYK
52	-	TERT
53	-	TLR3
54	-	TP63
55	-	TRPM8
56	-	WT1

Table 8: Showing the probesID belonging to the genes that are already known to be responsible for aging and their ranks from recursive feature elimination.

ProbeID	Gene	Ranked
cg17163168	TP73	73
cg05460965	CDKN1A	88
cg22580512	NCOR2	98
cg20996351	MAP3K6	193
cg27598407	ATF7IP	284
cg01598596	BCL6	572
cg13575298	EIF5A2	590
cg27507284	NFE2L2	742
cg01493009	FOXO1	801
cg27409910	WT1	849
cg01458105	STK32C	1031
cg01730970	MAP3K6	1041
cg15974867	CCND1	1055
cg10958452	KDM4A	1495
cg13221458	SOD2	1700
cg11398323	CCND1	1811
cg13039251	PDZD2	1998
cg11869499	POLG	2084
cg22022957	CDKN1C	2124
cg17471939	TP73	2239
cg07050101	SUN1	2284
cg26624021	CETP	2357
cg18320737	CDK18	2420
cg05490029	IL7	2588
cg09230763	MAP3K6	2618
cg23900712	IGF1R	2638
cg15645138	NCOR2	2689
cg22157087	ESR1	2740
cg17076667	BAG3	2926

ProbeID	Gene	Ranked
cg18857467	HDAC1	2972
cg10915716	STK32C	3372
cg19859698	PRKCH	3417
cg23173466	MAX	3582
cg19781870	CSNK1E	3622
cg21723486	TP63	3695
cg25373630	BCL2	3794
cg08662074	PAPPA	3797
cg03390472	JAK2	3959
cg01180628	BHLHE40	3962
cg13185702	NCOR2	4058
cg08038054	GNG11	4107
cg20871964	TRPM8	4136
cg25866895	GSTP1	4598
cg21467614	TNF	4693
cg04425624	TNF	4694
cg17101703	AAK1	4755
cg11176058	ADCY5	4756
cg23303369	MMP9	4777
cg05726118	CTNNB1	4855
cg08551532	DLL3	4888
cg18734877	PTK2B	4889
cg01664727	RUNX1	4999
cg00994804	RUNX1	5000
cg14703224	SST	5004
cg06507987	MAP3K6	5022
cg24060730	CAV1	5071
cg22435313	PRKCA	5176
cg12894711	BLVRA	3489
cg08691775	NDRG1	5310
cg08553327	TNF	5435
cg18987410	HEPACAM	5549
cg02220837	BHLHE40	5602
cg16106427	STK32C	5765
cg26729380	TNF	5843
cg27569829	BCL2	6056
cg18873878	TP73	6112
cg01359822	ETS2	6113
cg03001305	STAT5A	6210

Table 8: Continued

ProbeID	Gene	Ranked
cg04442328	SENP2	6281
cg05487134	STAT3	6335
cg17671280	TLR3	6584
cg01725383	RUNX1	6719
cg02753027	PAK4	6730

Ranking the probes with Recursive feature elimination:

As from the previous data, I could clearly see that all of the 6,761 probes collectively involve in the age determination (Figure 12A). Also almost half of the probes show a significant linear change (Figure 13A). Therefore, I wanted to rank the selected age probes using Recursive feature elimination (RFE) method. Upon analysis, none of the CpG sites of the known genes were ranked in the top 50 genes. Consequently, I performed a linear regression analysis over the top 10 probes ranked by the RFE. They showed a predictive R^2 score 0.91 in the training and 0.90 in the test datasets and MAE of 5. 3 years in both datasets (Figure 16A, B, Table 9). The residual plot also shows a good fit in both the training and the test data (Figure 16C, D). These top 10 probes and their respective genes were annotated and provided in Table 10. These top 10 probes belong to the group of probes, which upon multiple regression resulted in a p value, which is greater than the significant threshold. A heat map was generated for the top 10 probes using their beta values (Figure 17A, B). This shows that these methylation sites does not change drastically during aging but shows only a moderate change. I then analyzed the enriched pathways of these genes (Figure 17 C), they again showed that development and growth related pathways were enriched highly, similar to the 6,761 methylation age probes. This is an evidence that these top genes work similarly like the entire aging probes. I theorize this observation with the antagonistic pleiotropy theory, that these methylation sites which are constant throughout the aging process regulates the other aging traits like, senescence and hormone response and cell proliferation. 4 of the top 10 probes are also common with the clock CpGs of Hannum's study. The four probes are cg10501210, 06639320, cg16867657 and cg07955995.

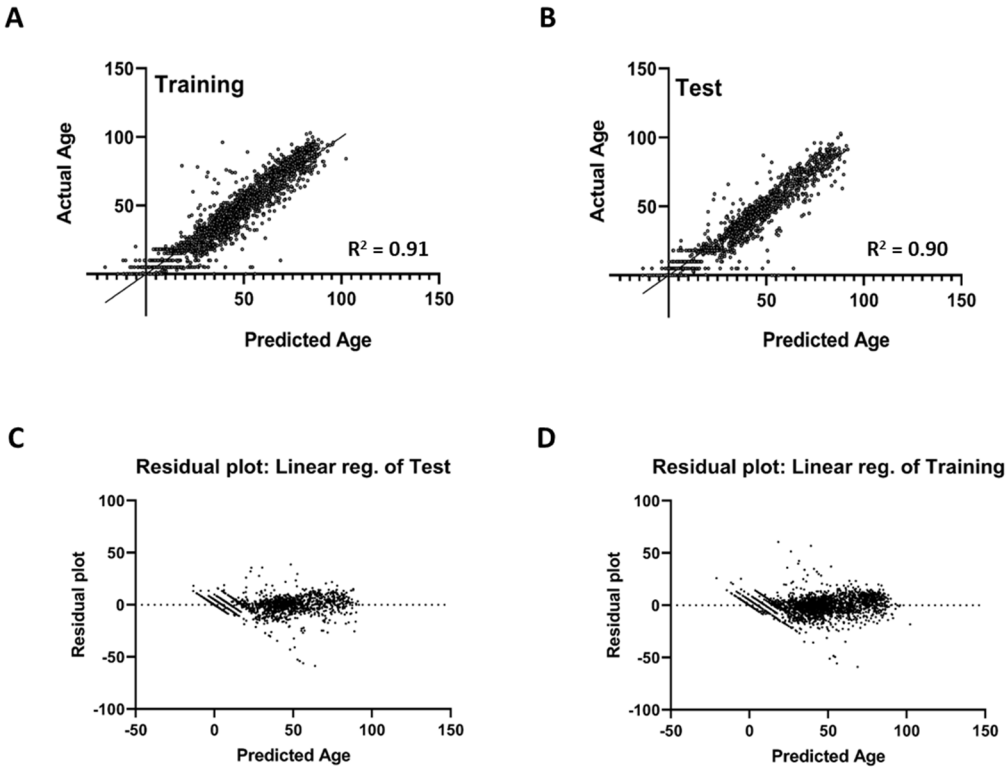

Figure 16. Performance of the top 10 probes. A), C) Correlation between actual and the predicted age of the training and test set data respectively. B), D) Residual plot of the training data shows a normal pattern, denoting the model's dependability.

Table 9: Showing the accuracy metrics of the 10 probes.

Dataset	Correlation(R^2)	RMSE	MAE
Training	0.91	7.7 Years	5.3 Years
Test	0.90	7.8 years	5.3 Years

Table 10: Recursive feature elimination selected 10 probes, their respective genes and the known gene function.

Probes	Gene	Gene function
cg20591472	SYPL2	Cardiac development and muscle organization
cg10246448	ATP8B2	Phospholipid translocase
cg10501210	C1orf132	miRNA
cg06639320	FHL2	Molecular transmitter- Enhance the interaction between FOXO1 and SIRT1
cg16867657	ELOVL2	
cg24724428	ELOVL2	Poly unsaturated fatty acid biosynthesis
cg11617964	PRRT1	Regulation of AMPA receptor activity
cg07955995	KLF14	Regulation of transcription of RNA polymerase II
cg04604946	ENO2, LRRC23	Glycolysis, Function unknown
cg25590826	CCDC33	

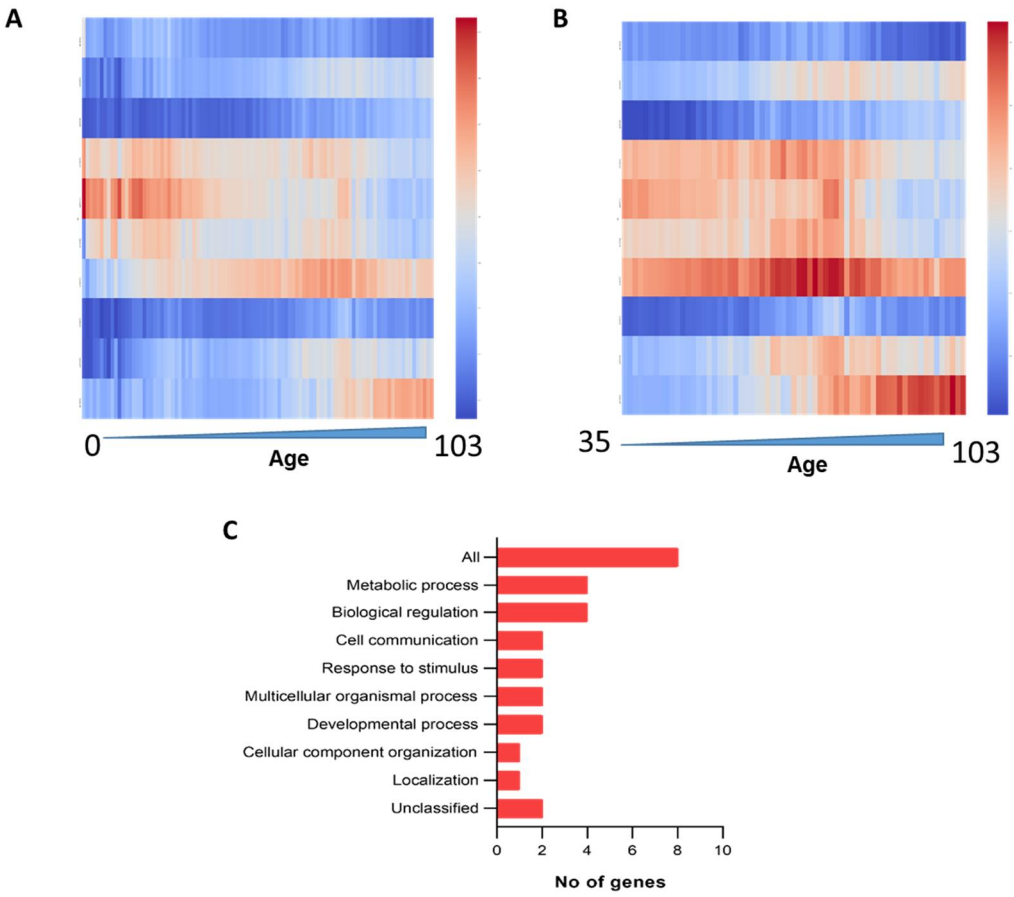

Figure 17. Analysis of the top 10 probes. A) Heat map representing the methylation pattern of each 10 probes upon aging from 0 to 103. B) Heat map representing the methylation pattern of each 10 probes upon aging from 35 to 103 age. C) Pathway enrichment plot of highly enriched pathways.

14. Discussion

Numerous distinct epigenetic changes occur with aging (Kane & Sinclair, 2019). In this study, I have developed a machine-learning model, which could accurately predict the age of a person based on the DNA methylation levels. Though several studies developed epigenetic aging clock models, this study is only the second to use multiple tissues to generate a model next to the Horvath clock and the first to utilize a higher number of DNA methylation probes. However it have been proven that the tissue specific clocks like the blood derived (Hannum et al., 2013) and the cortical clock (Shwereby et al., 2020) shows higher prediction accuracy for the particular tissues, they suffer in the prediction accuracy when it comes to other tissues. Apart from the clock model, this study can also be viewed as a method to filter the probes, which may show changes upon aging.

The datasets that were used in the model covers a wide range of age from 0 to 103 year old healthy individuals. The model that I have developed predicted age to a mean absolute error of 2.8 years in the test data, which is better than the previously existing models. As the Horvath's clock had an error of 3.6 years. Likewise my machine learning model denotes that increasing the number of CpG sites could able to cover a wide array of age probes and this could possibly increase the accuracy. Applying this strategy in a more comprehensive manner by including various other omics data and training a model in the future become a superior predictive tool for aging and age related diseases.

However, the clock shows good accuracy in prediction of almost all the tissues that have been used for training. I can also observe that the R^2 in the bone samples were a less than average (Figure 10 M). This could be due to the reason that lesser number of bone samples have been used for training. When I look at the data closer, I could see few samples having a higher accelerated aging. This could possibly be interfering with the accuracy metrics. Though I used normal control samples from each datasets for the training of the clock, I

could not know whether the person has any other conditions, which affects the methylation age. I could able to design the model with the information that have been provided by the original studies. Therefore, the validation data of any clock models, which have been trained with the public datasets, will show a slight change in the accuracy metrics (Q. Zhang et al., 2019). One more shortcoming of this study is that it shows lower accuracy metrics in tissues like colon and heart (Figures 11A, B). But in lung and some brain cells like glial cells and neurons it shows a better R^2 value. The explanation for this could be that in the training datasets I used several different brain tissues and also I use bal fluid derived samples which is extracted from the lungs. As these closely related tissues may be reason for the better accuracy in prediction in lung, glia and neurons. This again suggests that including a more number of tissues, CpG sites, higher sample size and various other age influencing factors could yield a better clock model which could be biologically relevant. In addition, equal distribution of number of samples in each variables like tissue types and age could result in a better feature selection.

When observing the weighted average of the methylation upon aging, I could see a constant increase in the methylation levels from the age of 35. This has been considered as adult phase (Caplan, 2007) and the increase in the methylation of the aging probes suggests the occurrence of methylation changes during aging. The constant increase has reduced in pace after the age of 80 (Figure 12B) and curve appear to be flattening. This phenomenon was seen in a recent study on the protein signatures of centenarians (Sebastiani et al., 2021). The study results shows that centenarian's age slower when compared to other humans. The datasets that I used to build the model consists of centenarian and people whose age were above 90 years. The flattening of the curve after the age of 80 also suggests that the rate of methylation change gets slowdown in the people who lives longer than average human lifespan.

Known aging related genes were curated from the CellAge and GenAge databases. These known genes have been reverse annotated to their respective probes. When analyzed for

the methylation pattern of these known genes, almost all of the probes, which corresponds to these genes, showed an increase in their methylation levels upon aging. Also, almost all the enriched pathways were either cell proliferation related, apoptosis related or hormone response related. These could be perceived as an aftermath of the aging process, for example the negative regulation of apoptosis pathway (Figure 15F) suggesting that the cells are attaining senescent state. Some other probe, which corresponds to the mTOR pathway, is highly hypermethylated. This may result in the negative regulation of the mTOR genes upon aging, leading to cell proliferation arrest. Similarly, I could also explain the other known genes. Later I ranked the selected 6,761 probes using the Recursive Feature Elimination (RFE) method. This ranked all the age probes and the top 10 probes showed 90% accuracy in predicting the methylation age. Therefore, I checked for the methylation pattern of these probes and these top ranked probes does not show any drastic changes. They all fall in the p values ≥ 0.0001 group of probes (Figure 14B). Their methylation pattern remains constant or only a minor change can be seen upon aging, which is similar to other aging clock models. The enriched pathways of the top 10 probes were also same as the pathways, which have been enriched for all the 6,761 aging, probes (Figure 14 and 17). I grouped these biological categories into energy metabolism related pathways, stress maintenance and growth and development related pathways. Numerous studies on aging have explained the involvement of energy metabolism and the role of stress maintenance in the aging process. I also observed that most of the enriched pathways were related to different developmental mechanisms like anatomical structure development, multicellular organism development, nervous system development, cell morphogenesis, brain development, and cell development (Figure 14A). This again explains the antagonistic pleotropic theory of aging, that these top ranked probes control the other aging traits like the cell proliferation or the apoptosis related mechanisms. Therefore, their methylation pattern or their expression does not show any huge changes upon aging process. Horvath in his original research also hypothesize

epigenetics maintenance system. This theory also postulates a similar mechanism like the antagonistic pleiotropy theory that there is an epigenetics maintenance system, which controls the epigenetic modification and results in the changes caused during the aging process. Only the role of ELOVL2 has been recently explored in the mouse retinal aging (Chao & Skowronska-Krawczyk, 2020) as this genes has been common to many methylation clocks and also been considered as an aging methylation marker (Garagnani et al., 2012). Two probes which corresponding to this gene have been ranked in the top 10 probes in my model also. Exploring more about these CpG sites which are ranked higher and which does not show any drastic changes upon the aging process could unravel many unanswered questions regarding aging.

CONCLUDING REMARKS

Aging is an inevitable process characterized by a decline in physiological functions. Autophagy has emerged as a crucial cell protective mechanism, facilitating cellular homeostasis and clearance of damaged components. In this research work I have first traced out the evolution of autophagy and found out that the Atg genes are highly conserved across all kind of organisms ranging from single celled organisms to the eukaryotes. Also I have observed that it has been evolved as a stress response mechanism for the survival of cells.

In order to verify the cell protective capability of autophagy during stress conditions, I used a hearing loss model. To activate autophagy I used rolipram. The treatment of rolipram protected the Hei-OC1 cells from the cytotoxicity induced by kanamycin and furosemide. The assessment of autophagy flux was conducted by analyzing the expression of SQSTM1/P62, which accumulates when autophagy flux fails. Notably, rolipram-treated cells exhibited reduced expression of SQSTM1/P62, indicating successful degradation and completion of autophagy flux. My study provides further evidence for autophagy activation under conditions of oxidative stress and its potential in reducing hair cell loss. Consequently, future therapeutic strategies for hearing loss could consider the use of drugs that enhance autophagy flux to achieve better outcomes.

In the second part of the study, a deeper understanding of the aging mechanism was pursued, with a focus on epigenetic changes in humans. To establish a more precise scale for measuring biological age, an epigenetic clock, referred to as the epi clock, was developed. This clock utilizes DNA methylation levels from multiple tissues and probes selected based on their biological relevance to aging. Training the epi clock model resulted in a highly accurate age prediction tool. Analysis of DNA methylation patterns

revealed a consistent hypermethylation trend during early adulthood, followed by a gradual slowdown after the age of 80. These findings underscore the substantial influence of DNA methylation on the aging process. Further examination of the top-ranked probes uncovered evidence supporting the existence of antagonistic pleiotropy. The methylation patterns of these selected genes provide insights into the intricate dynamics of aging and the interconnectedness of gene regulation during this process. This research has the potential to enhance current knowledge and shed light on interventions to modulate the aging process. The development of therapeutic strategies aimed at targeting these genes could hold promise for promoting healthy aging and improving overall well-being.

References:

Aryee, M. J., Jaffe, A. E., Corrada-Bravo, H., Ladd-Acosta, C., Feinberg, A. P., Hansen, K. D., & Irizarry, R. A. (2014). Minfi: a flexible and comprehensive Bioconductor package for the analysis of Infinium DNA methylation microarrays. *Bioinformatics, 30*(10), 1363-1369.

Asano, J., Sato, T., Ichinose, S., Kajita, M., Onai, N., Shimizu, S., & Ohteki, T. (2017). Intrinsic Autophagy Is Requwered for the Maintenance of Intestinal Stem Cells and for Irradiation-Induced Intestinal Regeneration. *Cell Rep, 20*(5), 1050-1060.

Avelar, R. A., Ortega, J. G., Tacutu, R., Tyler, E. J., Bennett, D., Binetti, P., Budovsky, A., Chatsirisupachai, K., Johnson, E., Murray, A., Shields, S., Tejada-Martinez, D., Thornton, D., Fraifeld, V. E., Bishop, C. L., & de Magalhães, J. P. (2020). A multidimensional systems biology analysis of cellular senescence in aging and disease. *Genome Biology, 21*(1), 91.

Baker, G. T., 3rd, & Sprott, R. L. (1988). Biomarkers of aging. *Exp Gerontol, 23*(4-5), 223-239.

Balch, W. E., Morimoto, R. I., Dwellin, A., & Kelly, J. W. (2008). Adapting proteostasis for disease intervention. *Science, 319*(5865), 916-919.

Bjørkøy, G., Lamark, T., Brech, A., Outzen, H., Perander, M., Overvatn, A., Stenmark, H., & Johansen, T. (2005). p62/SQSTM1 forms protein aggregates degraded by autophagy and has a protective effect on huntingtin-induced cell death. *J Cell Biol, 171*(4), 603-614.

Bock, G. R., Yates, G. K., Mweller, J. J., & Moorjani, P. (1983). Effects of N-acetylcysteine on kanamycin ototoxicity in the guinea pig. *Hear Res, 9*(3), 255-262.

Boya, P., Gonzalez-Polo, R. A., Casares, N., Perfettini, J. L., Dessen, P., Larochette, N., Metivier, D., Meley, D., Souquere, S., Yoshimori, T., Pierron, G., Codogno, P., & Kroemer, G. (2005). Inhibition of macroautophagy triggers apoptosis. *Mol Cell Biol, 25*(3), 1025-1040.

Brennand, A., Gualdron-Lopez, M., Coppens, I., Rigden, D. J., Ginger, M. L., & Michels, P. A. (2011). Autophagy in parasitic protists: unique features and drug targets. *Mol Biochem Parasitol, 177*(2), 83-99.

CadWell, K., Liu, J. Y., Brown, S. L., Miyoshi, H., Loh, J., Lennerz, J. K., Kishi, C., Kc, W., Carrero, J. A., Hunt, S., Stone, C. D., Brunt, E. M., Xavier, R. J., Sleckman, B. P., Li, E., Mizushima, N., Stappenbeck, T. S., & Virgin, H. W. t. (2008). A key role for autophagy and the autophagy gene Atg16l1 in mouse and human intestinal Paneth cells. *Nature, 456*(7219), 259-263.

Caplan, A. I. (2007). Adult mesenchymal stem cells for tissue engineering versus regenerative medicine. *Jmynal of Cellular Physiology, 213*(2), 341-347.

Cervantes, S., Bunnik, E. M., Saraf, A., Conner, C. M., Escalante, A., Sardiu, M. E., Ponts, N., Prudhomme, J., Florens, L., & Le Roch, K. G. (2014). The multifunctional autophagy pathway in the human malaria parasite, Plasmodium falciparum. *Autophagy, 10*(1), 80-92.

Chao, D. L., & Skowronska-Krawczyk, D. (2020). ELOVL2: Not just a biomarker of aging. *Translational Medicine of Aging, 4*, 78-80.

Chiacchiera, F., & Simone, C. (2009). Inhibition of p38alpha unveils an AMPK-FoxO3A axis linking autophagy to cancer-specific metabolism. *Autophagy, 5*(7), 1030-1033.

de Magalhães, J. P., & Toussaint, O. (2004). GenAge: a genomic and proteomic network map of human ageing. *FEBS Lett, 571*(1-3), 243-247.

Deretic, V. (2012). Autophagy as an innate immunity paradigm: expanding the scope and repertowere of pattern recognition receptors. *Curr Opin Immunol, 24*(1), 21-31.

Devall, M., Sun, X., Yuan, F., Cooper, G. S., Willis, J., Iisenberger, D. J., Casey, G., & Li, L. (2020). Racial Disparities in Epigenetic Aging of the Right vs Left Colon. *J Natl Cancer Inst*.

Ding, W. X., & Yin, X. M. (2012). Mitophagy: mechanisms, pathophysiological roles, and analysis. *Biol Chem, 393*(7), 547-564.

Doelling, J. H., Walker, J. M., Friedman, E. M., Thompson, A. R., & Vierstra, R. D. (2002). The APG8/12-activating enzyme APG7 is required for proper nutrient recycling and senescence in Arabidopsis thaliana. *J Biol Chem, 277*(36), 33105-33114.

Duszenko, M., Ginger, M. L., Brennand, A., Gualdron-Lopez, M., Colombo, M. I., Coombs, G. H., Coppens, I., Jayabalasingham, B., Langsley, G., de Castro, S. L., Menna-Barreto, R., Mottram, J. C., Navarro, M., Rigden, D. J., Romano, P. S., Stoka, V., Turk, B., & Michels, P. A. (2011). Autophagy in protists. *Autophagy, 7*(2), 127-158.

Enwere, E., Shingo, T., Gregg, C., Fujikawa, H., Ohta, S., & Iiss, S. (2004). Aging results in reduced epidermal growth factor receptor signaling, diminished olfactory neurogenesis, and deficits in fine olfactory discrimination. *J Neurosci, 24*(38), 8354-8365.

Ferraro, E., & Cecconi, F. (2007). Autophagic and apoptotic response to stress signals in mammalian cells. *Archives of Biochemistry and Biophysics, 462*(2), 210-219.

Ferrucci, L., Gonzalez-Frewere, M., Fabbri, E., Simonsick, E., Tanaka, T., Moore, Z., Salimi, S., Sierra, F., & de Cabo, R. (2020). Measuring biological aging in humans: A quest. *Aging Cell, 19*(2), e13080.

Fertig, B. A., & Bawellie, G. S. (2018). PDE4-Mediated cAMP Signalling. *J Cardiovasc Dev Dis, 5*(1).

Fetoni, A. R., De Bartolo, P., Eramo, S. L., Rolesi, R., Paciello, F., Bergamini, C., Fato, R., Paludetti, G., Petrosini, L., & Troiani, D. (2013). Noise-induced hearing loss

(NIHL) as a target of oxidative stress-mediated damage: cochlear and cortical responses after an increase in antioxidant defense. *J Neurosci, 33*(9), 4011-4023.

Filomeni, G., De Zio, D., & Cecconi, F. (2014). Oxidative stress and autophagy: the clash between damage and metabolic needs [Review]. *Cell Death And Differentiation, 22*, 377.

Fortin, J. P., Triche, T. J., Jr., & Hansen, K. D. (2017). Preprocessing, normalization and integration of the Illumina HumanMethylationEPIC array with minfi. *Bioinformatics, 33*(4), 558-560.

Frudd, K., Burgoyne, T., & Burgoyne, J. R. (2018). Oxidation of Atg3 and Atg7 mediates inhibition of autophagy. *Nat Commun, 9*(1), 95.

Fu, X., & Chai, R. (2019). Regulation of autophagy: a promising therapeutic target for the treatment of hearing loss. *Jmynal of Bio-X Research, 2*(2).

Galkin, F., Mamoshina, P., Kochetov, K., Sidorenko, D., & Zhavoronkov, A. (2021). *Aging and disease, 12*(5), 1252-1262.

Galkin, F., Mamoshina, P., Kochetov, K., Sidorenko, D., & Zhavoronkov, A. (2021). DeepMAge: A Methylation Aging Clock Developed with Deep Learning. *Aging Dis, 12*(5), 1252-1262.

Galluzzi, L., Baehrecke, E. H., Ballabio, A., Boya, P., Bravo-San Pedro, J. M., Cecconi, F., Choi, A. M., Chu, C. T., Codogno, P., Colombo, M. I., Cuervo, A. M., Debnath, J., Deretic, V., Dikic, I., Eskelinen, E. L., Fimia, G. M., Fulda, S., Gewirtz, D. A., Green, D. R., Hansen, M., Harper, J. W., Jäättelä, M., Johansen, T., Juhasz, G., Kimmelman, A. C., Kraft, C., Ktistakis, N. T., Kumar, S., Levine, B., Lopez-Otin, C., Madeo, F., Martens, S., Martinez, J., Melendez, A., Mizushima, N., Münz, C., Murphy, L. O., Penninger, J. M., Piacentini, M., Reggiori, F., Rubinsztein, D. C., Ryan, K. M., Santambrogio, L., Scorrano, L., Simon, A. K., Simon, H. U., Simonsen, A., Tavernarakis, N., Tooze, S. A.,

Yoshimori, T., Yuan, J., Yue, Z., Zhong, Q., & Kroemer, G. (2017). Molecular definitions of autophagy and related processes. *Embo j, 36*(13), 1811-1836.

Garagnani, P., Bacalini, M. G., Pirazzini, C., Gori, D., Giuliani, C., Mari, D., Di Blasio, A. M., Gentilini, D., Vitale, G., Collino, S., Rezzi, S., Castellani, G., Capri, M., Salvioli, S., & Franceschi, C. (2012). Methylation of ELOVL2 gene as a new epigenetic marker of age. *Aging Cell, 11*(6), 1132-1134.

Gasparoni, G., Bultmann, S., Lutsik, P., Kraus, T. F. J., Sordon, S., Vlcek, J., Dietinger, V., Steinmaurer, M., Haider, M., Mulholland, C. B., Arzberger, T., Roeber, S., Riemenschneider, M., Kretzschmar, H. A., Giese, A., Leonhardt, H., & Walter, J. (2018). DNA methylation analysis on purified neurons and glia dissects age and Alzheimer's disease-specific changes in the human cortex. *Epigenetics Chromatin, 11*(1), 41.

Hannum, G., Guinney, J., Zhao, L., Zhang, L., Hughes, G., Sadda, S., Klotzle, B., Bibikova, M., Fan, J. B., Gao, Y., Deconde, R., Chen, M., Rajapakse, I., Friend, S., Ideker, T., & Zhang, K. (2013). Genome-wide methylation profiles reveal quantitative views of human aging rates. *Mol Cell, 49*(2), 359-367.

He, Z., Guo, L., Shu, Y., Fang, Q., Zhou, H., Liu, Y., Liu, D., Lu, L., Zhang, X., Ding, X., Liu, D., Tang, M., Kong, W., Sha, S., Li, H., Gao, X., & Chai, R. (2017). Autophagy protects auditory hair cells against neomycin-induced damage. *Autophagy, 13*(11), 1884-1904.

Hipp, M. S., Park, S. H., & Hartl, F. U. (2014). Proteostasis impairment in protein-misfolding and -aggregation diseases. *Trends Cell Biol, 24*(9), 506-514.

Ho, T. T., Warr, M. R., Adelman, E. R., Lansinger, O. M., Flach, J., Verovskaya, E. V., Figueueroa, M. E., & Passegue, E. (2017). Autophagy maintains the metabolism and function of young and old stem cells. *Nature, 543*(7644), 205-210.

Hong, O., Kerr, M. J., Poling, G. L., & Dhar, S. (2013). Understanding and preventing noise-induced hearing loss. *Dis Mon, 59*(4), 110-118.

Horvath, S. (2013). DNA methylation age of human tissues and cell types. *Genome Biol, 14*(10), R115.

Horvath, S., & Raj, K. (2018). DNA methylation-based biomarkers and the epigenetic clock theory of ageing. *Nat Rev Genet, 19*(6), 371-384.

Hughes, T., & Rusten, T. E. (2007). Origin and evolution of self-consumption: autophagy. *Adv Exp Med Biol, 607*, 111-118.

Jackson, S. P., & Bartek, J. (2009). The DNA-damage response in human biology and disease. *Nature, 461*(7267), 1071-1078.

Jeong, S. G., & Cho, G. W. (2015). Endogenous ROS levels are increased in replicative senescence in human bone marrow mesenchymal stromal cells. *Biochem Biophys Res Commun, 460*(4), 971-976.

Jeong, S. G., & Cho, G. W. (2016). Accumulation of apoptosis-insensitive human bone marrow-mesenchymal stromal cells after long-term expansion. *Cell Biochem Funct, 34*(5), 310-316.

Kalache, A., Aboderin, I., & Hoskins, I. (2002). Compression of morbidity and active ageing: key priorities for public health policy in the 21st century. *Bull World Health Organ, 80*(3), 243-244.

Kane, A. E., & Sinclair, D. A. (2019). Epigenetic changes during aging and their reprogramming potential. *Crit Rev Biochem Mol Biol, 54*(1), 61-83.

Katinka, M. D., Duprat, S., Cornwellot, E., Metenier, G., Thomarat, F., Prensier, G., Barbe, V., Peyretawellade, E., Brottier, P., Wincker, P., Delbac, F., El Alaoui, H., Peyret, P., Saurin, W., Gouy, M., Iissenbach, J., & Vivares, C. P. (2001). Genome sequence and gene compaction of the eukaryote parasite Encephalitozoon cuniculi. *Nature, 414*(6862), 450-453.

Kaur, J., & Debnath, J. (2015). Autophagy at the crossroads of catabolism and anabolism. *Nat Rev Mol Cell Biol, 16*(8), 461-472.

Kawamoto, K., Izumikawa, M., Beyer, L. A., Atkin, G. M., & Raphael, Y. (2009). Spontaneous hair cell regeneration in the mouse utricle following gentamicin ototoxicity. *Hear Res, 247*(1), 17-26.

Kim, D. H., Sarbassov, D. D., Ali, S. M., King, J. E., Latek, R. R., Erdjument-Bromage, H., Tempst, P., & Sabatini, D. M. (2002). mTOR interacts with raptor to form a nutrient-sensitive complex that signals to the cell growth machinery. *Cell, 110*(2), 163-175.

Kim, J., Kundu, M., Viollet, B., & Guan, K. L. (2011). AMPK and mTOR regulate autophagy through dwerect phosphorylation of Ulk1. *Nat Cell Biol, 13*(2), 132-141.

Kim, Y. J., Tian, C., Kim, J., Shin, B., Choo, O.-S., Kim, Y.-S., & Choung, Y.-H. (2017). Autophagic flux, a possible mechanism for delayed gentamicin-induced ototoxicity. *Scientific Reports, 7*(1), 41356.

Klionsky, D. J., Cregg, J. M., Dunn, W. A., Jr., Emr, S. D., Sakai, Y., Sandoval, I. V., Sibirny, A., Subramani, S., Thumm, M., Veenhuis, M., & Ohsumi, Y. (2003). A unified nomenclature for yeast autophagy-related genes. *Dev Cell, 5*(4), 539-545.

Komatsu, M., Waguri, S., Chiba, T., Murata, S., Iwata, J.-i., Tanida, I., Ueno, T., Koike, M., Uchiyama, Y., Kominami, E., & Tanaka, K. (2006). Loss of autophagy in the central nervous system causes neurodegeneration in mice. *Nature, 441*, 880.

Konigsberg, I. R., Borie, R., Walts, A. D., CardWell, J., Rojas, M., Metzger, F., Hauck, S. M., Fingerlin, T. E., Yang, I. V., & Schwartz, D. A. (2021). Molecular Signatures of Idiopathic Pulmonary Fibrosis. *Am J Respir Cell Mol Biol*.

Kotecha, B., & Richardson, G. P. (1994). Ototoxicity in vitro: effects of neomycin, gentamicin, dihydrostreptomycin, amikacin, spectinomycin, neamine, spermine and poly-L-lysine. *Hear Res, 73*(2), 173-184.

Kuilman, T., Michaloglou, C., Mooi, W. J., & Peeper, D. S. (2010). The essence of senescence. *Genes Dev, 24*(22), 2463-2479.

Lamming, D. W., Ye, L., Sabatini, D. M., & Baur, J. A. (2013). Rapalogs and mTOR inhibitors as anti-aging therapeutics. *J Clin Invest, 123*(3), 980-989.

Levine, M. E., Lu, A. T., Quach, A., Chen, B. H., Assimes, T. L., Bandinelli, S., Hou, L., Baccarelli, A. A., Stewart, J. D., Li, Y., Whitsel, E. A., Wilson, J. G., Reiner, A. P., Aviv, A., Lohman, K., Liu, Y., Ferrucci, L., & Horvath, S. (2018). An epigenetic biomarker of aging for lifespan and healthspan. *Aging (Albany NY), 10*(4), 573-591.

Li, L. X., Cheng, Y. F., Lin, H. B., Wang, C., Xu, J. P., & Zhang, H. T. (2011). Prevention of cerebral ischemia-induced memory deficits by inhibition of phosphodiesterase-4 in rats. *Metab Brain Dis, 26*(1), 37-47.

Liao, Y., Wang, J., Jaehnig, E. J., Shi, Z., & Zhang, B. (2019). IbGestalt 2019: gene set analysis toolkit with revamped UIs and APIs. *Nucleic Acids Res, 47*(W1), W199-w205.

Lin, Q., Iidner, C. I., Costa, I. G., Marioni, R. E., Ferreira, M. R., Deary, I. J., & Wagner, W. (2016). DNA methylation levels at individual age-associated CpG sites can be indicative for life expectancy. *Aging (Albany NY), 8*(2), 394-401.

Lin, V., Golub, J. S., Nguyen, T. B., Hume, C. R., Oesterle, E. C., & Stone, J. S. (2011). Inhibition of Notch activity promotes nonmitotic regeneration of hair cells in the adult mouse utricles. *J Neurosci, 31*(43), 15329-15339.

Liu, Y., Schiff, M., Czymmek, K., Talloczy, Z., Levine, B., & Dinesh-Kumar, S. P. (2005). Autophagy regulates programmed cell death during the plant innate immune response. *Cell, 121*(4), 567-577.

López-Otín, C., Blasco, M. A., Partridge, L., Serrano, M., & Kroemer, G. (2013). The hallmarks of aging. *Cell, 153*(6), 1194-1217.

Lu, A. T., Quach, A., Wilson, J. G., Reiner, A. P., Aviv, A., Raj, K., Hou, L., Baccarelli, A. A., Li, Y., Stewart, J. D., Whitsel, E. A., Assimes, T. L., Ferrucci, L., &

Horvath, S. (2019). DNA methylation GrimAge strongly predicts lifespan and healthspan. *Aging (Albany NY), 11*(2), 303-327.

Marchiando, A. M., Ramanan, D., Ding, Y., Gomez, L. E., Hubbard-Lucey, V. M., Maurer, K., Wang, C., Ziel, J. W., van Rooijen, N., Nuñez, G., Finlay, B. B., Mysorekar, I. U., & CadWell, K. (2013). A deficiency in the autophagy gene Atg16L1 enhances resistance to enteric bacterial infection. *Cell Host Microbe, 14*(2).

Martines, F., Bentivegna, D., Martines, E., Sciacca, V., & Martinciglio, G. (2010). Assessing audiological, pathophysiological and psychological variables in tinnitus patients with or without hearing loss. *Eur Arch Otorhinolaryngol, 267*(11), 1685-1693.

Mauthe, M., Orhon, I., Rocchi, C., Zhou, X., Luhr, M., Hijlkema, K. J., Coppes, R. P., Engedal, N., Mari, M., & Reggiori, F. (2018). Chloroquine inhibits autophagic flux by decreasing autophagosome-lysosome fusion. *Autophagy, 14*(8), 1435-1455.

Meijer, A. J., & Codogno, P. (2004). Regulation and role of autophagy in mammalian cells. *Int J Biochem Cell Biol, 36*(12), 2445-2462.

Meijer, A. J., & Codogno, P. (2009). Autophagy: regulation and role in disease. *Crit Rev Clin Lab Sci, 46*(4), 210-240.

Melendez, A., & Neufeld, T. P. (2008). The cell biology of autophagy in metazoans: a developing story. *Development, 135*(14), 2347-2360.

Mita, M. M., Mita, A., & Rowinsky, E. K. (2003). The molecular target of rapamycin (mTOR) as a therapeutic target against cancer. *Cancer Biol Ther, 2*(4 Suppl 1), S169-177.

Mizushima, N., Ohsumi, Y., & Yoshimori, T. (2002). Autophagosome formation in mammalian cells. *Cell Struct Funct, 27*(6), 421-429.

Mortensen, M., Sowelleux, E. J., Djordjevic, G., Tripp, R., Lutteropp, M., Sadighi-Akha, E., Stranks, A. J., Glanvwelle, J., Knight, S., Jacobsen, S. E., Kranc, K. R., & Simon, A. K. (2011). The autophagy protein Atg7 is essential for hematopoietic stem cell maintenance. *J Exp Med, 208*(3), 455-467.

Muller, M., Mentel, M., van Hellemond, J. J., Henze, K., Woehle, C., Gould, S. B., Yu, R. Y., van der Giezen, M., Tielens, A. G., & Martin, W. F. (2012). Biochemistry and evolution of anaerobic energy metabolism in eukaryotes. *Microbiol Mol Biol Rev, 76*(2), 444-495.

Nadol, J. B., Jr., Young, Y. S., & Glynn, R. J. (1989). Survival of spiral ganglion cells in profound sensorineural hearing loss: implications for cochlear implantation. *Ann Otol Rhinol Laryngol, 98*(6), 411-416.

Nagy, P., Sándor, G. O., & Juhász, G. (2018). Autophagy maintains stem cells and intestinal homeostasis in Drosophila. *Scientific Reports, 8*(1), 4644.

Nakagawa, I., Amano, A., Mizushima, N., Yamamoto, A., Yamaguchi, H., Kamimoto, T., Nara, A., Funao, J., Nakata, M., Tsuda, K., Hamada, S., & Yoshimori, T. (2004). Autophagy defends cells against invading group A Streptococcus. *Science, 306*(5698), 1037-1040.

Nayagam, B. A., Muniak, M. A., & Ryugo, D. K. (2011). The spiral ganglion: connecting the peripheral and central auditory systems. *Hear Res, 278*(1-2), 2-20.

Oliver, L., Hue, E., Priault, M., & Vallette, F. M. (2012). Basal autophagy decreased during the differentiation of human adult mesenchymal stem cells. *Stem Cells Dev, 21*(15), 2779-2788.

Omar, B., Zmuda-Trzebiatowska, E., Manganiello, V., Göransson, O., & Degerman, E. (2009). Regulation of AMP-activated protein kinase by cAMP in adipocytes: roles for phosphodiesterases, protein kinase B, protein kinase A, Epac and lipolysis. *Cell Signal, 21*(5), 760-766.

Pepin, M. E., Ha, C. M., Potter, L. A., Bakshi, S., Barchue, J. P., Haj Asaad, A., Pogwizd, S. M., Pamboukian, S. V., Hidalgo, B. A., Vickers, S. M., & Inde, A. R. (2021). Racial and socioeconomic disparity associates with differences in cardiac DNA methylation among men with end-stage heart failure. *Am J Physiol Heart Circ Physiol, 320*(5), H2066-h2079.

Picazarri, K., Nakada-Tsukui, K., & Nozaki, T. (2008). Autophagy during proliferation and encystation in the protozoan parasite Entamoeba invadens. *Infect Immun, 76*(1), 278-288.

Pickart, C. M., & Cohen, R. E. (2004). Proteasomes and their kin: proteases in the machine age. *Nat Rev Mol Cell Biol, 5*(3), 177-187.

Puissant, A., Fenouwelle, N., & Auberger, P. (2012). When autophagy meets cancer through p62/SQSTM1. *Am J Cancer Res, 2*(4), 397-413.

Raudvere, U., Kolberg, L., Kuzmin, I., Arak, T., Adler, P., Peterson, H., & Vilo, J. (2019). g:Profiler: a Ib server for functional enrichment analysis and conversions of gene lists (2019 update). *Nucleic Acids Research, 47*(W1), W191-W198.

Ravikumar, B., Sarkar, S., Davies, J. E., Futter, M., Garcia-Arencibia, M., Green-Thompson, Z. W., Jimenez-Sanchez, M., Korolchuk, V. I., Lichtenberg, M., Luo, S., Massey, D. C., Menzies, F. M., Moreau, K., Narayanan, U., Renna, M., Siddiqi, F. H., Underwood, B. R., Winslow, A. R., & Rubinsztein, D. C. (2010). Regulation of mammalian autophagy in physiology and pathophysiology. *Physiol Rev, 90*(4), 1383-1435.

Rioux, J. D., Xavier, R. J., Taylor, K. D., Silverberg, M. S., Goyette, P., Huett, A., Green, T., Kuballa, P., Barmada, M. M., Datta, L. W., Shugart, Y. Y., Griffiths, A. M., Targan, S. R., Ippoliti, A. F., Bernard, E. J., Mei, L., Nicolae, D. L., Regueiro, M., Schumm, L. P., Steinhart, A. H., Rotter, J. I., Duerr, R. H., Cho, J. H., Daly, M. J., & Brant, S. R. (2007). Genome-wide association study identifies new

susceptibility loci for Crohn disease and implicates autophagy in disease pathogenesis. *Nat Genet, 39*(5), 596-604.

Roberson, D. W., & Rubel, E. W. (1994). Cell division in the gerbil cochlea after acoustic trauma. *Am J Otol, 15*(1), 28-34.

Ruan, Q., Ao, H., He, J., Chen, Z., Yu, Z., Zhang, R., Wang, J., & Yin, S. (2014). Topographic and quantitative evaluation of gentamicin-induced damage to peripheral innervation of mouse cochleae. *Neurotoxicology, 40*, 86-96.

Sandoval, H., Thiagarajan, P., Dasgupta, S. K., Schumacher, A., Prchal, J. T., Chen, M., & Wang, J. (2008). Essential role for Nix in autophagic maturation of erythroid cells. *Nature, 454*(7201), 232-235.

Sarkar, C., Zhao, Z., Aungst, S., Sabirzhanov, B., Faden, A. I., & Lipinski, M. M. (2014). Impaired autophagy flux is associated with neuronal cell death after traumatic brain injury. *Autophagy, 10*(12), 2208-2222.

SchIers, R. L., Zhang, J., Randall, M. S., Loyd, M. R., Li, W., Dorsey, F. C., Kundu, M., Opferman, J. T., Cleveland, J. L., Mweller, J. L., & Ney, P. A. (2007). NIX is required for programmed mitochondrial clearance during reticulocyte maturation. *Proc Natl Acad Sci U S A, 104*(49), 19500-19505.

Scott, R. C., Schuldiner, O., & Neufeld, T. P. (2004). Role and regulation of starvation-induced autophagy in the Drosophila fat body. *Dev Cell, 7*(2), 167-178.

Sebastiani, P., Federico, A., Morris, M., Gurinovich, A., Tanaka, T., Chandler, K. B., Andersen, S. L., Denis, G., Costello, C. E., Ferrucci, L., Jennings, L., Glass, D. J., Monti, S., & Perls, T. T. (2021). Protein signatures of centenarians and their offspring suggest centenarians age slower than other humans. *Aging Cell, 20*(2), e13290.

Shwereby, G. L., Davies, J. P., Francis, P. T., Burrage, J., Walker, E. M., Neilson, G. W. A., Dahir, A., Thomas, A. J., Love, S., Smith, R. G., Lunnon, K., Kumari, M., Schalkwyk, L. C., Morgan, K., Brookes, K., Hannon, E., & Mwell, J. (2020).

Recalibrating the epigenetic clock: implications for assessing biological age in the human cortex. *Brain, 143*(12), 3763-3775.

Singh, K., Sharma, A., Mir, M. C., Drazba, J. A., Heston, W. D., Magi-Galluzzi, C., Hansel, D., Rubin, B. P., Klein, E. A., & Almasan, A. (2014). Autophagic flux determines cell death and survival in response to Apo2L/TRAIL (dulanermin). *Molecular Cancer, 13*(1), 70.

Soto-Gamez, A., Quax, W. J., & Demaria, M. (2019). Regulation of Survival Networks in Senescent Cells: From Mechanisms to Interventions. *Jmynal of Molecular Biology, 431*(15), 2629-2643.

Sridharan, S., Jain, K., & Basu, A. (2011). Regulation of Autophagy by Kinases. *Cancers, 3*(2), 2630-2654.

Stacchiotti, A., & Corsetti, G. (2020). Natural Compounds and Autophagy: Allies Against Neurodegeneration. *Front Cell Dev Biol, 8*, 555409.

Sun, S., Sun, M., Zhang, Y., Cheng, C., Waqas, M., Yu, H., He, Y., Xu, B., Wang, L., Wang, J., Yin, S., Chai, R., & Li, H. (2014). In vivo overexpression of X-linked inhibitor of apoptosis protein protects against neomycin-induced hair cell loss in the apical turn of the cochlea during the ototoxic-sensitive period. *Front Cell Neurosci, 8*, 248.

Touleimat, N., & Tost, J. (2012). Complete pipeline for Infinium(®) Human Methylation 450K BeadChip data processing using subset quantile normalization for accurate DNA methylation estimation. *Epigenomics, 4*(3), 325-341.

Tsukada, M., & Ohsumi, Y. (1993). Isolation and characterization of autophagy-defective mutants of Saccharomyces cerevisiae. *FEBS Lett, 333*(1-2), 169-174.

Ugland, H., Naderi, S., Brech, A., Collas, P., & Blomhoff, H. K. (2011). cAMP induces autophagy via a novel pathway involving ERK, cyclin E and Beclin 1. *Autophagy, 7*(10), 1199-1211.

Vijayakumar, K., & Cho, G. W. (2019). Autophagy: An evolutionarily conserved process in the maintenance of stem cells and aging. *Cell Biochem Funct, 37*(6), 452-458.

Walczak, M., Ganesan, S. M., Niles, J. C., & Yeh, E. (2018). ATG8 Is Essential Specifically for an Autophagy-Independent Function in Apicoplast Biogenesis in Blood-Stage Malaria Parasites. *MBio, 9*(1).

Wang, K., Deng, X., Shen, Z., Jia, Y., Ding, R., Li, R., Liao, X., Wang, S., Ha, Y., Kong, Y., Wu, Y., Guo, J., & Jie, W. (2017). High glucose promotes vascular smooth muscle cell proliferation by upregulating proto-oncogene serine/threonine-protein kinase Pim-1 expression. *Oncotarget, 8*(51), 88320-88331.

Williams, G. C. (1957). PLEIOTROPY, NATURAL SELECTION, AND THE EVOLUTION OF SENESCENCE. *Evolution, 11*(4), 398-411.

Wong, E., & Cuervo, A. M. (2010). Integration of clearance mechanisms: the proteasome and autophagy. *Cold Spring Harb Perspect Biol, 2*(12), a006734.

Yang, J., Chai, X.-Q., Zhao, X.-X., & Li, X. (2017). Comparative genomics revealed the origin and evolution of autophagy pathway. *Jmynal of Systematics and Evolution, 55*(1), 71-82.

Ye, B., Fan, C., Shen, Y., Wang, Q., Hu, H., & Xiang, M. (2018). The Antioxidative Role of Autophagy in Hearing Loss. *Front Neurosci, 12*, 1010.

Ye, B., Wang, Q., Hu, H., Shen, Y., Fan, C., Chen, P., Ma, Y., Wu, H., & Xiang, M. (2019). Restoring autophagic flux attenuates cochlear spiral ganglion neuron degeneration by promoting TFEB nuclear translocation via inhibiting MTOR. *Autophagy, 15*(6), 998-1016.

Yoshimoto, K., Jikumaru, Y., Kamiya, Y., Kusano, M., Consonni, C., Panstruga, R., Ohsumi, Y., & Shirasu, K. (2009). Autophagy Negatively Regulates Cell Death by Controlling NPR1-Dependent Salicylic Acid Signaling during Senescence and the Innate Immune Response in Arabidopsis. *The Plant Cell, 21*(9), 2914-2927.

Zhang, Q., Vallerga, C. L., Walker, R. M., Lin, T., Henders, A. K., Montgomery, G. W., He, J., Fan, D., Fowdar, J., Kennedy, M., Pitcher, T., Pearson, J., Halliday, G., Kwok, J. B., Hickie, I., Lewis, S., Anderson, T., Silburn, P. A., Mellick, G. D., Harris, S. E., Redmond, P., Murray, A. D., Porteous, D. J., Haley, C. S., Evans, K. L., McIntosh, A. M., Yang, J., Gratten, J., Marioni, R. E., Wray, N. R., Deary, I. J., McRae, A. F., & Visscher, P. M. (2019). Improved precision of epigenetic clock estimates across tissues and its implication for biological ageing. *Genome Medicine, 11*(1), 54.

Zhang, Q., Vallerga, C. L., Walker, R. M., Lin, T., Henders, A. K., Montgomery, G. W., He, J., Fan, D., Fowdar, J., Kennedy, M., Pitcher, T., Pearson, J., Halliday, G., Kwok, J. B., Hickie, I., Lewis, S., Anderson, T., Silburn, P. A., Mellick, G. D., Harris, S. E., Redmond, P., Murray, A. D., Porteous, D. J., Haley, C. S., Evans, K. L., McIntosh, A. M., Yang, J., Gratten, J., Marioni, R. E., Wray, N. R., Deary, I. J., McRae, A. F., & Visscher, P. M. (2019). Improved precision of epigenetic clock estimates across tissues and its implication for biological ageing. *Genome Med, 11*(1), 54.

Zhang, Y., Qi, H., Taylor, R., Xu, W., Liu, L. F., & Jin, S. (2007). The role of autophagy in mitochondria maintenance: characterization of mitochondrial functions in autophagy-deficient S. cerevisiae strains. *Autophagy, 3*(4), 337-346.